Energy conservation issues in the numerical solution of the semilinear wave equation

L. Brugnano[a], G. Frasca Caccia[a,*], F. Iavernaro[b]

[a] *Dipartimento di Matematica e Informatica "U. Dini", Università di Firenze, Firenze, Italy*
[b] *Dipartimento di Matematica, Università di Bari, Bari, Italy*

ARTICLE INFO

ABSTRACT

In this paper we discuss energy conservation issues related to the numerical solution of the semilinear wave equation. As is well known, this problem can be cast as a Hamiltonian system that may be autonomous or not, depending on the prescribed boundary conditions. We relate the conservation properties of the original problem to those of its semi-discrete version obtained by the method of lines. Subsequently, we show that the very same properties can be transferred to the solutions of the fully discretized problem, obtained by using energy-conserving methods in the HBVMs (Hamiltonian Boundary Value Methods) class. Similar arguments hold true for different types of Hamiltonian partial differential equations, e.g., the nonlinear Schrödinger equation.

© 2015 Elsevier Inc. All rights reserved.

1. Introduction

In this paper we discuss energy-conservation issues for the semilinear wave equation, though the approach can be extended to different kinds of *Hamiltonian partial differential equations* (like, e.g., the nonlinear Schrödinger equation). For simplicity, but without loss of generality, we shall consider the following 1D case,

$$
\begin{aligned}
u_{tt}(x,t) &= u_{xx}(x,t) - f'(u(x,t)), \quad (x,t) \in (0,1) \times (0,\infty), \\
u(x,0) &= \psi_0(x), \\
u_t(x,0) &= \psi_1(x), \quad x \in (0,1),
\end{aligned}
\tag{1}
$$

coupled with suitable boundary conditions. As usual, subscripts denote partial derivatives. In (1), the functions f, ψ_0 and ψ_1 are supposed to be suitably regular and such that they define a regular solution $u(x,t)$ (f' denotes the derivative of f). The problem is completed by assigning suitable boundary conditions which we shall, at first, assume to be periodic,

$$
u(0,t) = u(1,t), \quad t > 0.
\tag{2}
$$

In such a case, we will assume that ψ_0, ψ_1, and f are such that the resulting solution also satisfies

$$
u_x(0,t) = u_x(1,t), \quad t > 0.
\tag{3}
$$

Later on, we shall also consider the case of Dirichlet boundary conditions,

$$
u(0,t) = \varphi_0(t), \quad u(1,t) = \varphi_1(t), \quad t > 0,
\tag{4}
$$

---

* Corresponding author. Tel.: +39 3343341368; fax: +39 055 2751 452.
   E-mail address: frasca@math.unifi.it (G. Frasca Caccia).

and Neumann boundary conditions,

$$u_x(0, t) = \phi_0(t), \quad u_x(1, t) = \phi_1(t), \quad t > 0,\tag{5}$$

with $\varphi_0(t)$, $\varphi_1(t)$, $\phi_0(t)$, and $\phi_1(t)$ suitably regular. We set

$$v = u_t,\tag{6}$$

and define the Hamiltonian functional

$$\mathcal{H}[u, v](t) = \int_0^1 \left[\frac{1}{2}v^2(x, t) + \frac{1}{2}u_x^2(x, t) + f(u(x, t))\right]dx \equiv \int_0^1 E(x, t)\,dx.\tag{7}$$

As is well known, we can rewrite (1) as the infinite-dimensional Hamiltonian system (for brevity, we neglect the arguments of the functions u and v)

$$\mathbf{z}_t = J\frac{\delta\mathcal{H}}{\delta\mathbf{z}},\tag{8}$$

where

$$J = \begin{pmatrix} 0 & 1 \\ -1 & 0 \end{pmatrix}, \quad \mathbf{z} = \begin{pmatrix} u \\ v \end{pmatrix},\tag{9}$$

and

$$\frac{\delta\mathcal{H}}{\delta\mathbf{z}} = \left(\frac{\delta\mathcal{H}}{\delta u}, \frac{\delta\mathcal{H}}{\delta v}\right)^\top\tag{10}$$

is the functional derivative of $\mathcal{H}$. This latter is defined as follows: given a generic functional in the form

$$\mathcal{L}[q] = \int_a^b L(x, q(x), q'(x))dx,$$

its functional derivative $\frac{\delta\mathcal{L}}{\delta q}$ is defined by requiring that, for every function $\xi(x)$,

$$\int_a^b \frac{\delta\mathcal{L}}{\delta q} \cdot \xi\,dx \equiv \lim_{\varepsilon \to 0} \frac{\mathcal{L}[q + \varepsilon\xi] - \mathcal{L}[q]}{\varepsilon} = \left.\frac{d}{d\varepsilon}\mathcal{L}[q + \varepsilon\xi]\right|_{\varepsilon=0}.$$

In particular, by considering a function ξ vanishing at a and b, one obtains:

$$\int_a^b \frac{\delta\mathcal{L}}{\delta q} \cdot \xi\,dx = \left[\frac{d}{d\varepsilon}\int_a^b L(x, q + \varepsilon\xi, q' + \varepsilon\xi')dx\right]_{\varepsilon=0} = \int_a^b \left(\frac{\partial L}{\partial q}\xi + \frac{\partial L}{\partial q'}\xi'\right)dx$$

$$= \int_a^b \left[\frac{\partial L}{\partial q}\xi + \frac{d}{dx}\left(\frac{\partial L}{\partial q'}\xi\right) - \left(\frac{d}{dx}\frac{\partial L}{\partial q'}\right)\xi\right]dx$$

$$= \int_a^b \left[\frac{\partial L}{\partial q}\xi - \left(\frac{d}{dx}\frac{\partial L}{\partial q'}\right)\xi\right]dx = \int_a^b \left(\frac{\partial L}{\partial q} - \left(\frac{d}{dx}\frac{\partial L}{\partial q'}\right)\right)\xi\,dx.$$

Consequently,

$$\frac{\delta\mathcal{L}}{\delta q} = \frac{\partial L}{\partial q} - \left(\frac{d}{dx}\frac{\partial L}{\partial q'}\right).\tag{11}$$

Exploiting (11), one easily verifies that (8)–(10) are equivalent to (1):

$$\mathbf{z}_t = \begin{pmatrix} u_t \\ v_t \end{pmatrix} = J\frac{\delta\mathcal{H}}{\delta\mathbf{z}} = \begin{pmatrix} \frac{\delta\mathcal{H}}{\delta v} \\ -\frac{\delta\mathcal{H}}{\delta u} \end{pmatrix} = \begin{pmatrix} v \\ u_{xx} - f'(u) \end{pmatrix},$$

or

$$u_t(x, t) = v(x, t), \quad (x, t) \in (0, 1) \times (0, \infty),$$
$$v_t(x, t) = u_{xx}(x, t) - f'(u(x, t)),\tag{12}$$

that is, the first-order formulation of the first equation in (1).

The numerical treatment of Hamiltonian PDEs such as (1) has been the subject of an intense research activity during the past decade (see, e.g., [9] for a survey). The extension of ideas and tools related to geometric integration of ordinary differential equations (ODEs) has led to the definition and analysis of various structure preserving algorithms suitable for specific or general classes of PDEs. Two main lines of investigations are based on a multisymplectic reformulation of the equations or their semi-discretization by means of the method of lines.

Multisymplectic structures generalize the classical Hamiltonian structure of a Hamiltonian ODE by assigning a distinct symplectic operator for each unbounded space direction and time [6]. A clear advantage of this approach is that it allows for an easy generalization from symplectic to multisymplectic integration. Multisymplectic integrators are numerical methods which precisely conserve a discrete space-time symplectic structure of Hamiltonian PDEs [7,40,41,52,57,68] (a backward error analysis of such schemes may be found in [58,59,72]).

In the method of lines approach, the spatial derivatives are usually approximated by finite differences or by discrete Fourier transform and the resulting system is then integrated in time by a suitable ODE integrator. Spectral methods have revealed very good potentialities especially in the case of periodic boundary conditions [39,82].[1] For weakly nonlinear term f' in (1), the modulated Fourier expansion technique [49, Chapter XIII] has been adapted to both the semi-discretized and the full-discretized systems to state long-time near conservation of energy, momentum, and actions [33,50]. In general, quoting [78, p. 187], if the PDEs are of Hamiltonian type, (…) the space discretization should be carried out in such a way that the resulting system of ODEs is Hamiltonian (for a suitable Poisson bracket) and the time integration should also be carried out by a symplectic or Poisson integrator. This approach (which we shall consider here), has been the subject of many researches (e.g., [26,42,48,51,65,67,73,76]). Whichever is the considered discretization, the main aim is that of keeping conserved discrete counterparts of continuous invariants, as done, e.g., in [44,45,53,69,70], with the so called *discrete variational derivative method*. Additional references are [38,66,80].

In this paper, we focus our attention on numerical techniques able to provide a full discretization of the original system with the discrete energy behaving consistently with the energy function associated with (1). More precisely, to approximate the second order spatial derivative, we use either a central finite difference or a spectral expansion, and then we derive a semi-discrete analogue of the conservation law associated with the energy density. As is well known, whatever the boundary conditions, the rate of change of the energy density integrated over an interval depends only on the flux through its endpoints. We show that the use of an energy-conserving method to discretize the time assures a precise reproduction of the above mentioned conservation law of the semi-discrete model. In particular, if there is no net flux into or out of the interval, then the integrated energy density is precisely conserved, meaning that it remains constant over time. Some of the presented results, in the case of periodic boundary conditions, are already known (see, e.g., [26,73,76]). Nevertheless, these authors mainly focus on the conservation properties of the semi-discrete model, and consider accurate symplectic integrators for their solution. Instead, we are here more interested in a precise conservation of the semi-discrete energy and, because of this reason, we consider energy-conserving methods. Moreover, the algebraic form in which we cast the semi-discrete problem is quite concise, and allows for a simple extension to the case where the boundary conditions are not periodic.

A popular strategy for the numerical treatment of generic boundary conditions is that of considering a *Summation By Parts* (*SBP*) operator in space, consisting of a basic centered difference scheme suitably modified in a number of points near the boundary in order to assure stability and high order (see [46,71,79]). The boundary conditions can be then imposed by means of projection methods (see [74,75]) or *Simultaneous Approximation Term* (*SAT*) methods adding penalty terms in the semi-discrete problem (see [28,43]). Nevertheless, since the SBP operators are not symmetric, this approach is not able to return a Hamiltonian semi-discretization of the continuous problem and, therefore, it does not fit the main goal of this paper: showing the benefits which one could have when the energy of a semi-discrete version of the original Hamiltonian problem is exactly (or at least practically) conserved.

When the problem is coupled with the periodic boundary conditions (2), the integral of E (see (7)) is indeed a conserved quantity and one obtains *energy conservation* (see, e.g., [64]). Therefore, it makes sense to look for a corresponding conservation property, when numerically solving the problem (as done, e.g., in [26,73,76]). Nevertheless, also in the other cases (i.e., (4) and (5)), which are of interest in applications, the qualitative properties of the solution can be suitably reproduced in the discrete approximation by slightly generalizing the arguments. In fact, in all cases, one may derive a semi-discrete problem which turns out to be Hamiltonian, and whose Hamiltonian mimics a semi-discrete energy which is exactly conserved. Consequently, it makes sense to use energy-conserving methods for their numerical solution.

Energy conserving methods, in turn, have been the subject of many investigations, in the ODE setting, during the past years: we quote, as an example, *discrete gradient methods* [61,62], *time finite elements* [3,4], the *average vector field method* [30,31,77] and its generalizations [47]. This latter method has also been considered in the PDE setting (e.g., [29]). In particular, we shall here consider the energy-conserving methods in the class of *Hamiltonian Boundary Value Methods (HBVMs)* [12,15–20], which are methods based on the concept of *discrete line integral*, as defined in [54–56]. Such methods have been also generalized to the case of different conservative problems [11,14,21,22,25] and, more recently, they have been used for numerically solving Hamiltonian boundary value problems [1].

With this premise, the paper is organized as follows:

- We study, at first, the discrete problems derived by a finite-difference spatial discretization. In particular, in Section 2 we study the case in which problem (1) is completed by the periodic boundary conditions (2); the case of Dirichlet boundary conditions (4) will be the subject of Section 3; at last, the case of Neumann boundary conditions (5) will be examined in Section 4.
- We then study, in Section 5, the case where a Fourier–Galerkin space discretization is considered, when periodic boundary conditions are prescribed. Also, higher order finite-difference approximations are sketched.

---

[1] They have been also applied to multisymplectic PDEs [8,32,81].

- In Section 6 we study the efficient implementation of the proposed energy-conserving methods. In Section 7 we report a few numerical tests, whereas Section 8 contains a few concluding remarks.
- Finally, in the Appendix we sketch the way how the whole approach can be extended to different kinds of Hamiltonian PDEs. In particular, we consider the nonlinear Schrödinger equation.

2. The case of periodic boundary conditions

By considering that the time derivative of the integrand function $E(x, t)$ defined at (7) satisfies (see (12))

$$
\begin{aligned}
E_t(x, t) &= v(x, t)v_t(x, t) + u_x(x, t)u_{xt}(x, t) + f'(u(x, t))u_t(x, t) \\
&= v(x, t)(u_{xx}(x, t) - f'(u(x, t))) + u_x(x, t)v_x(x, t) + f'(u(x, t))v(x, t) \\
&= v(x, t)u_{xx}(x, t) + u_x(x, t)v_x(x, t) = (u_x(x, t)v(x, t))_x \equiv -F_x(x, t),
\end{aligned}
$$

one derives the conservation law:

$$
E_t(x, t) + F_x(x, t) = 0, \quad \text{with} \quad F(x, t) = -u_x(x, t)v(x, t). \tag{13}
$$

Consequently, because of the periodic boundary conditions (2) (and (3)), one obtains

$$
\dot{\mathcal{H}}[\mathbf{z}](t) = \int_0^1 E_t(x, t)\mathrm{d}x = [u_x(x, t)v(x, t)]_{x=0}^1 = 0,
$$

where, as usual, the dot denotes the time derivative. Therefore (7) is a conserved quantity, so that at $t = h$ one has:

$$
\mathcal{H}[\mathbf{z}](h) = \mathcal{H}[\mathbf{z}](0).
$$

We also recast the Hamiltonian function in a more convenient form to be used in the sequel. In case of the periodic boundary conditions (2), from (7) one has

$$
\begin{aligned}
\mathcal{H}[\mathbf{z}](t) &\equiv \int_0^1 E(x, t)\,\mathrm{d}x = \int_0^1 \left[\frac{1}{2}v^2(x, t) + \frac{1}{2}u_x^2(x, t) + f(u(x, t))\right]\mathrm{d}x \\
&= \int_0^1 \left[\frac{1}{2}v^2(x, t) + \frac{1}{2}[(u(x, t)u_x(x, t))_x - u(x, t)u_{xx}(x, t)] + f(u(x, t))\right]\mathrm{d}x \\
&= \int_0^1 \left[\frac{1}{2}v^2(x, t) - \frac{1}{2}u(x, t)u_{xx}(x, t) + f(u(x, t))\right]\mathrm{d}x + \frac{1}{2}\underbrace{\left[u(x, t)u_x(x, t)\right]_{x=0}^1}_{=0} \\
&= \int_0^1 \left[\frac{1}{2}v^2(x, t) - \frac{1}{2}u(x, t)u_{xx}(x, t) + f(u(x, t))\right]\mathrm{d}x,
\end{aligned} \tag{14}
$$

where $[uu_x]_{x=0}^1 = 0$ because of the periodic boundary conditions (2) (and (3)).

2.1. Semi-discretization

For numerically solving problem (1)–(2), let us introduce the following discretization of the space variable,

$$
x_i = i\Delta x, \quad i = 0, \dots, N, \quad \Delta x = 1/N,
$$

and the vectors:

$$
\mathbf{x} = \begin{pmatrix} x_0 \\ \vdots \\ x_{N-1} \end{pmatrix}, \quad \mathbf{q}(t) = \begin{pmatrix} u_0(t) \\ \vdots \\ u_{N-1}(t) \end{pmatrix}, \quad \mathbf{p}(t) = \begin{pmatrix} v_0(t) \\ \vdots \\ v_{N-1}(t) \end{pmatrix} \in \mathbb{R}^N,
$$

with

$$
u_i(t) \approx u(x_i, t), \quad v_i(t) \approx v(x_i, t) \equiv u_t(x_i, t). \tag{15}
$$

Because of the periodic boundary conditions (2), we also set:

$$
u_N(t) \equiv u_0(t), \quad u_{-1}(t) \equiv u_{N-1}(t), \quad t \geq 0.
$$

Approximating the second derivative in (12) as

$$
u_{xx}(x_i, t) \approx \frac{u_{i+1}(t) - 2u_i(t) + u_{i-1}(t)}{\Delta x^2}, \quad i = 0, \dots, N-1, \tag{16}
$$

yields the following semi-discrete problem

$$
\dot{\mathbf{q}} = \mathbf{p}, \tag{17}
$$

$$\dot{\mathbf{p}} = -\frac{1}{\Delta x^2} T_N \mathbf{q} - f'(\mathbf{q}), \quad t > 0,$$

with the initial condition

$$\mathbf{q}(0) = \psi_0(\mathbf{x}), \quad \mathbf{p}(0) = \psi_1(\mathbf{x}), \qquad (18)$$

(with an obvious meaning for $f'(\mathbf{q})$, $\psi_0(\mathbf{x})$, and $\psi_1(\mathbf{x})$) and the following approximation of the Hamiltonian (14),

$$H \equiv H(\mathbf{q}, \mathbf{p}) = \Delta x \left[\frac{\mathbf{p}^\top \mathbf{p}}{2} + \frac{\mathbf{q}^\top T_N \mathbf{q}}{2 \Delta x^2} + \mathbf{e}^\top f(\mathbf{q}) \right], \qquad (19)$$

where T_N is a circulant matrix,[2]

$$T_N = \begin{pmatrix} 2 & -1 & & & -1 \\ -1 & \ddots & \ddots & & \\ & \ddots & \ddots & \ddots & \\ & & \ddots & \ddots & -1 \\ -1 & & & -1 & 2 \end{pmatrix} \in \mathbb{R}^{N \times N}, \qquad (20)$$

and

$$\mathbf{e} = (1 \quad \ldots \quad 1)^\top \in \mathbb{R}^N. \qquad (21)$$

Problem (17) is clearly Hamiltonian. In fact, one has

$$\dot{\mathbf{q}} = \frac{1}{\Delta x} \nabla_{\mathbf{p}} H, \quad \dot{\mathbf{p}} = -\frac{1}{\Delta x} \nabla_{\mathbf{q}} H,$$

or, by introducing the vector

$$\mathbf{y} = \begin{pmatrix} \mathbf{q} \\ \mathbf{p} \end{pmatrix},$$

one obtains the more compact form

$$\dot{\mathbf{y}} = J_N \nabla H(\mathbf{y}), \quad \text{with} \quad J_N = \frac{1}{\Delta x} \begin{pmatrix} 0 & I_N \\ -I_N & 0 \end{pmatrix}, \qquad (22)$$

where here and in the sequel we use, when appropriate, the notation $H(\mathbf{y}) = H(\mathbf{q}, \mathbf{p})$. Consequently,

$$\dot{H}(\mathbf{y}) = \nabla H(\mathbf{y})^\top \dot{\mathbf{y}} = \nabla H(\mathbf{y})^\top J_N \nabla H(\mathbf{y}) = 0,$$

because J_N is skew-symmetric. One then concludes that the discrete approximation (19)–(14) is a conserved quantity for the semi-discrete problem (22). Writing (19) in componentwise form,

$$H(\mathbf{q}, \mathbf{p}) = \Delta x \sum_{i=0}^{N-1} \left(\frac{1}{2} v_i^2 - u_i \frac{u_{i-1} - 2u_i + u_{i+1}}{2 \Delta x^2} + f(u_i) \right), \qquad (23)$$

one notices that (19) is nothing but the approximation of (14) via the composite trapezoidal rule (provided that the second derivative u_{xx} has been previously approximated as indicated at (16), and taking into account the periodic boundary conditions (2)). Consequently, one sees that (23) is a $O(\Delta x^2)$ approximation to (14).

2.2. Full discretization

Problem (22) can be discretized by using a HBVM(k, s) method which allows for a (at least *practical*) conservation of (19), by using a suitably large value $k \geq s$ [20], as is shown in the sequel. Let us study the approximation to the solution over the time interval $[0, h]$, representing the very first step of the numerical approximation, to be repeated subsequently. For this purpose, we shall consider the orthonormal polynomial basis over the interval $[0,1]$, $\{P_j\}$, given by the shifted and scaled Legendre polynomials:

$$\deg P_i = i, \quad \int_0^1 P_i(x) P_j(x) \mathrm{d}x = \delta_{ij}, \quad \forall i, j \geq 0,$$

δ_{ij} being the Kronecker symbol. Let us then expand the right-hand side of (22) along this basis, thus obtaining

$$\dot{\mathbf{y}}(ch) = \sum_{j \geq 0} \gamma_j(\mathbf{y}) P_j(c), \quad c \in [0, 1], \qquad (24)$$

---

[2] Because of the periodic boundary conditions (2).

with

$$\gamma_j(\mathbf{y}) = \int_0^1 J_N \nabla H(\mathbf{y}(\tau h)) P_j(\tau) \mathrm{d}\tau, \quad j \geq 0. \tag{25}$$

It is possible to prove the following result [20].

Lemma 1. *Assume* $\nabla H(\mathbf{y}(\,\cdot\,))$ *can be expanded in Taylor series at* 0. *Then:*

$$\gamma_j(\mathbf{y}) = O(h^j) \in \mathbb{R}^{2N}, \quad j = 0, 1, \ldots.$$

Setting the initial condition (see (1))

$$\mathbf{y}_0 = \begin{pmatrix} \psi_0(\mathbf{x}) \\ \psi_1(\mathbf{x}) \end{pmatrix}, \tag{26}$$

with $\psi_j(\mathbf{x})$, $j = 0, 1$, the vector whose entries are given by $\psi_j(x_i)$, the solution of (24)–(26) is then formally given by:

$$\mathbf{y}(ch) = \mathbf{y}_0 + h \sum_{j \geq 0} \gamma_j(\mathbf{y}) \int_0^c P_j(x) \mathrm{d}x, \quad c \in [0, 1]. \tag{27}$$

In order to obtain a polynomial approximation $\sigma \in \Pi_s$ to (27), we consider the following *truncated* initial value problem [20],

$$\dot{\sigma}(ch) = \sum_{j=0}^{s-1} \gamma_j(\sigma) P_j(c), \quad c \in [0, 1], \quad \sigma(0) = \mathbf{y}_0, \tag{28}$$

where $\gamma_j(\sigma)$ is still given by (25) by replacing $\mathbf{y}$ with σ. The polynomial approximation to (27) is then formally given by:

$$\sigma(ch) = \mathbf{y}_0 + h \sum_{j=0}^{s-1} \gamma_j(\sigma) \int_0^c P_j(x) \mathrm{d}x, \quad c \in [0, 1].$$

The use of a Gauss Legendre quadrature formula of order $2k$ to approximate the integral defining $\gamma_j(\sigma)$ (see (25)) would give [20]

$$\begin{aligned} \gamma_j(\sigma) &= \int_0^1 J_N \nabla H(\sigma(\tau h)) P_j(\tau) \mathrm{d}\tau \\ &= \underbrace{\sum_{\ell=1}^k b_\ell P_j(c_\ell) J_N \nabla H(\sigma(c_\ell h))}_{=\hat{\gamma}_j(\sigma)} + \Delta_j(h) \equiv \hat{\gamma}_j(\sigma) + \Delta_j(h), \end{aligned} \tag{29}$$

with

$$\Delta_j(h) = O(h^{2k-j}) \in \mathbb{R}^{2N}, \quad j = 0, \ldots, s-1. \tag{30}$$

In such a case, however, we have a different polynomial $\mathbf{u} \in \Pi_s$, in place of σ, solution of the problem

$$\dot{\mathbf{u}}(ch) = \sum_{j=0}^{s-1} \hat{\gamma}_j(\mathbf{u}) P_j(c), \quad c \in [0, 1], \quad \mathbf{u}(0) = \mathbf{y}_0, \tag{31}$$

$$\hat{\gamma}_j(\mathbf{u}) = \sum_{i=1}^k b_i P_j(c_i) J_N \nabla H(\mathbf{u}(c_i h)), \quad j = 0, \ldots, s-1,$$

instead of (28): this latter problem defines a HBVM(k, s) method.

If $H(\mathbf{q}, \mathbf{p})$ in (19) is a polynomial of degree $\nu \geq 2$ (which means that $f \in \Pi_\nu$),[3] and k is an integer such that

$$k \geq \frac{1}{2} \nu s \quad \Leftrightarrow \quad \nu \leq \frac{2k}{s}, \tag{32}$$

we can exactly compute the integrals $\gamma_j(\sigma)$ by means of a Gauss-quadrature formula of order $2k$, so that $\mathbf{u} \equiv \sigma$ and, then:

$$\begin{aligned} H(\sigma(h)) - H(\sigma(0)) &= h \int_0^1 \nabla H(\sigma(\tau h))^\top \dot{\sigma}(\tau h) \mathrm{d}\tau \\ &= h \int_0^1 \nabla H(\sigma(\tau h))^\top \sum_{j=0}^{s-1} P_j(\tau) \gamma_j(\sigma) \mathrm{d}\tau = h \Delta x^2 \sum_{j=0}^{s-1} \gamma_j(\sigma)^\top J_N \gamma_j(\sigma) = 0, \end{aligned} \tag{33}$$

---

[3] Indeed, H contains at least a quadratic term.

due to the fact that J_N is skew-symmetric. If f, and then H, is not a polynomial, by taking into account (22) and (29)–(31), the error on the Hamiltonian H, at $t = h$, is:

$$
\begin{aligned}
H(\mathbf{u}(h)) - H(\mathbf{u}(0)) &= h \int_0^1 \nabla H(\mathbf{u}(\tau h))^\top \dot{\mathbf{u}}(\tau h) \mathrm{d}\tau \\
&= h \int_0^1 \nabla H(\mathbf{u}(\tau h))^\top \sum_{j=0}^{s-1} P_j(\tau)\big(\gamma_j(\mathbf{u}) - \Delta_j(h)\big) \mathrm{d}\tau \\
&= h \Delta x^2 \sum_{j=0}^{s-1} \left[\overbrace{\gamma_j(\mathbf{u})^\top J_N \gamma_j(\mathbf{u})}^{=0} - \gamma_j(\mathbf{u})^\top J_N \Delta_j(h) \right] \\
&= h \underbrace{\Delta x \cdot N}_{=1} \cdot O(h^{2k}) \equiv O(h^{2k+1}),
\end{aligned}
\tag{34}
$$

where the last equality follows from Lemma 1 and (30). Consequently, choosing k large enough allows us to approximate the Hamiltonian H within full machine accuracy. Summing up all the previous arguments and taking into account the results in [20], the following results can be proved.

Theorem 1. *The HBVM(k, s) method (31) is the k-stage Runge–Kutta method with tableau*

$$
\begin{array}{c|c}
\mathbf{c} & \mathcal{I}\mathcal{P}^\top \Omega \\
\hline
& \mathbf{b}^\top
\end{array}
\quad with \quad
\begin{cases}
\mathbf{b} = (b_1 \ldots b_k)^\top, \\
\mathbf{c} = (c_1 \ldots c_k)^\top,
\end{cases}
\quad
\Omega = \begin{pmatrix} b_1 & & \\ & \ddots & \\ & & b_k \end{pmatrix},
$$

$$
and \quad \mathcal{P} = (P_{j-1}(c_i)), \quad \mathcal{I} = \left(\int_0^{c_i} P_{j-1}(x)\mathrm{d}x \right) \in \mathbb{R}^{k \times s}.
\tag{35}
$$

Theorem 2. *Assume $k \geq s$, and define $\mathbf{y}_1 = \mathbf{u}(h)$ as the new approximation to $\mathbf{y}(h)$ provided by a HBVM(k, s) method used with stepsize h. One then obtains:*

$$
\mathbf{y}_1 - \mathbf{y}(h) = O(h^{2s+1}),
$$

that is the method has order $2s$. Moreover, assuming that f is suitably regular:

$$
H(\mathbf{y}_1) - H(\mathbf{y}_0) = \begin{cases} 0, & if\ f \in \Pi_\nu\ and\ (32)\ holds\ true, \\ O(h^{2k+1}), & otherwise. \end{cases}
$$

Remark 1. From this result, it follows that one can always obtain the conservation of the discrete Hamiltonian (19) when f is a polynomial, by choosing k large enough. Moreover, as (34) suggests, also in the non-polynomial case, a *practical* conservation of (19) can be gained by choosing k large enough, so that the approximation is within round-off errors. As we shall see in Section 6, this is not a severe drawback, since the discrete problem generated by a HBVM(k, s) method has dimension s, independently of k (see also [12,18,20]).

3. The case of Dirichlet boundary conditions

Let us now consider the case when the considered problem is given by (1) with the boundary conditions (4). By repeating similar steps as done in (14), one obtains:

$$
\begin{aligned}
\mathcal{H}[\mathbf{z}](t) &= \int_0^1 E(x, t)\mathrm{d}x \equiv \int_0^1 \left[\frac{1}{2}v(x, t)^2 + \frac{1}{2}u_x(x, t)^2 + f(u(x, t)) \right] \mathrm{d}x \\
&= \int_0^1 \left[\frac{1}{2}v(x, t)^2 + \frac{1}{2}[(u(x, t)u_x(x, t))_x - u(x, t)u_{xx}(x, t)] + f(u(x, t)) \right] \mathrm{d}x \\
&= \int_0^1 \left[\frac{1}{2}v(x, t)^2 - \frac{1}{2}u(x, t)u_{xx}(x, t) + f(u(x, t)) \right] \mathrm{d}x + \frac{1}{2}[u(x, t)u_x(x, t)]_{x=0}^1 \\
&= \int_0^1 \left[\frac{1}{2}v(x, t)^2 - \frac{1}{2}u(x, t)u_{xx}(x, t) + f(u(x, t)) \right] \mathrm{d}x + \frac{1}{2}[u(1, t)u_x(1, t) - u(0, t)u_x(0, t)].
\end{aligned}
\tag{36}
$$

Moreover, $\mathcal{H}[\mathbf{z}]$ is no more conserved because formally (13) still holds true and, then, one obtains (see also (7), and taking into account the boundary conditions (4)):

$$
\dot{\mathcal{H}}[\mathbf{z}](t) = \int_0^1 E_t(x, t)\mathrm{d}x = [u_x(x, t)v(x, t)]_{x=0}^1 = u_x(1, t)\varphi_1'(t) - u_x(0, t)\varphi_0'(t).
\tag{37}
$$

Eq. (37) may be interpreted as the instant variation of the energy which is released or gained by the system at time t. Thus, the continuous Hamiltonian (7), though no more conserved, has a *prescribed variation in time*. From (37), at $t = h$ one easily obtains:

$$\mathcal{H}[\mathbf{z}](h) - \mathcal{H}[\mathbf{z}](0) = \int_0^h \dot{\mathcal{H}}[\mathbf{z}](t)\mathrm{d}t = \int_0^h [u_x(1, t)\varphi_1'(t) - u_x(0, t)\varphi_0'(t)]\mathrm{d}t, \tag{38}$$

and we have conservation when the Dirichlet boundary conditions are constant, e.g., homogeneous. In particular, in the latter case the conservation of the Hamiltonian may also assure the well-posedness of the problem, provided that the initial conditions are such that the Hamiltonian is bounded and the nonlinear term in the equation satisfies suitable assumptions. As an example, let us assume f bounded from below, that is $f(u) \geq -L, L \geq 0, \forall u \in \mathbb{R}$. Consequently, by exploiting the well-known Poincaré inequality (see, e.g., [36, p. 289]), there exists a constant $C > 0$ independent of u such that:

$$\|u(x, t)\|_{L^2([0,1])}^2 \leq C(\|v(x, t)\|_{L^2([0,1])}^2 + \|u_x(x, t)\|_{L^2([0,1])}^2) = 2C(\mathcal{H}[u, v](t) - \int_0^1 f(u(x, t))\mathrm{d}x) \leq 2C(\mathcal{H}[u, v](0) + L).$$

3.1. Semi-discretization

In order for numerically solving problem (1)–(4), let us introduce the following discretization of the space variable,

$$x_i = i\Delta x, \quad i = 0, \ldots, N + 1 \quad \Delta x = 1/(N + 1), \tag{39}$$

and the vectors:

$$\mathbf{x} = \begin{pmatrix} x_1 \\ \vdots \\ x_N \end{pmatrix}, \quad \mathbf{q}(t) = \begin{pmatrix} u_1(t) \\ \vdots \\ u_N(t) \end{pmatrix}, \quad \mathbf{p}(t) = \begin{pmatrix} v_1(t) \\ \vdots \\ v_N(t) \end{pmatrix} \in \mathbb{R}^N, \tag{40}$$

with $u_i(t)$ and $v_i(t)$ formally defined as in (15). Approximating the second derivatives in (12) as follows,

$$u_{xx}(x_i, t) \approx \frac{u_{i+1}(t) - 2u_i(t) + u_{i-1}(t)}{\Delta x^2}, \quad i = 1, \ldots, N,$$

and, moreover,

$$u_x(1, t) \approx \frac{u_{N+1}(t) - u_N(t)}{\Delta x}, \quad u_x(0, t) \approx \frac{u_1(t) - u_0(t)}{\Delta x}, \tag{41}$$

we then arrive at the following semi-discrete version of (36):

$$H = \Delta x \sum_{i=1}^N \left(\frac{1}{2}v_i^2 - u_i \frac{u_{i-1} - 2u_i + u_{i+1}}{2\Delta x^2} + f(u_i) \right) + \frac{1}{2}\left[u_{N+1}\frac{u_{N+1} - u_N}{\Delta x} - u_0\frac{u_1 - u_0}{\Delta x} \right]. \tag{42}$$

Moreover, because of the boundary conditions (4), one has:

$$u_0(t) = \varphi_0(t), \quad u_{N+1}(t) = \varphi_1(t), \tag{43}$$

so that we obtain the following semi-discrete approximation to the Hamiltonian (36):

$$H = \Delta x \sum_{i=1}^N \left(\frac{1}{2}v_i^2 - u_i \frac{u_{i-1} - 2u_i + u_{i+1}}{2\Delta x^2} + f(u_i) \right) + \varphi_1 \frac{\varphi_1 - u_N}{2\Delta x} + \varphi_0 \frac{\varphi_0 - u_1}{2\Delta x}.$$

H can be rewritten in vector form as

$$H \equiv H(\mathbf{q}, \mathbf{p}, t) = \Delta x \left[\frac{\mathbf{p}^\top \mathbf{p}}{2} + \frac{\mathbf{q}^\top T_N \mathbf{q}}{2\Delta x^2} + \mathbf{e}^\top f(\mathbf{q}) \right] + \frac{\boldsymbol{\varphi}(t)^\top \boldsymbol{\varphi}(t)}{2\Delta x} - \frac{\mathbf{q}^\top \boldsymbol{\varphi}(t)}{\Delta x}, \tag{44}$$

where $\mathbf{e}$ has been defined in (21) and, moreover:

$$T_N = \begin{pmatrix} 2 & -1 & & & \\ -1 & \ddots & \ddots & & \\ & \ddots & \ddots & \ddots & \\ & & \ddots & \ddots & -1 \\ & & & -1 & 2 \end{pmatrix} \in \mathbb{R}^{N \times N}, \quad \boldsymbol{\varphi}(t) = \begin{pmatrix} \varphi_0(t) \\ 0 \\ \vdots \\ 0 \\ \varphi_1(t) \end{pmatrix} \in \mathbb{R}^N. \tag{45}$$

With reference to (44)–(45), the corresponding semi-discrete problem is then given by:

$$\dot{\mathbf{q}} = \mathbf{p} \equiv \frac{1}{\Delta x}\nabla_{\mathbf{p}}H, \quad t > 0, \tag{46}$$

$$\dot{\mathbf{p}} = -\frac{1}{\Delta x^2} T_N \mathbf{q} + \frac{1}{\Delta x^2} \boldsymbol{\varphi} - f'(\mathbf{q}) \equiv -\frac{1}{\Delta x} \nabla_{\mathbf{q}} H,$$

which is clearly Hamiltonian, though the Hamiltonian (44) is now non-autonomous, because of the boundary conditions (4).

In order for conveniently handling this problem, we at first transform (46) into an enlarged *autonomous* Hamiltonian system, by introducing the following auxiliary conjugate scalar variables,

$$\tilde{q} \equiv t, \quad \tilde{p}, \tag{47}$$

and the augmented Hamiltonian (compare with (44)),

$$\tilde{H}(\mathbf{q}, \mathbf{p}, \tilde{q}, \tilde{p}) = \Delta x \left[\frac{\mathbf{p}^\top \mathbf{p}}{2} + \frac{\mathbf{q}^\top T_N \mathbf{q}}{2\Delta x^2} + \mathbf{e}^\top f(\mathbf{q}) \right] + \frac{\boldsymbol{\varphi}(\tilde{q})^\top \boldsymbol{\varphi}(\tilde{q})}{2\Delta x} - \frac{\mathbf{q}^\top \boldsymbol{\varphi}(\tilde{q})}{\Delta x} + \tilde{p}$$

$$\equiv H(\mathbf{q}, \mathbf{p}, \tilde{q}) + \tilde{p}. \tag{48}$$

The dynamical system corresponding to this new Hamiltonian function is, for $t > 0$:

$$\dot{\mathbf{q}} = \mathbf{p} \equiv \frac{1}{\Delta x} \nabla_{\mathbf{p}} \tilde{H},$$

$$\dot{\mathbf{p}} = -\frac{1}{\Delta x^2} T_N \mathbf{q} + \frac{1}{\Delta x^2} \boldsymbol{\varphi} - f'(\mathbf{q}) \equiv -\frac{1}{\Delta x} \nabla_{\mathbf{q}} \tilde{H},$$

$$\frac{\mathrm{d}}{\mathrm{d}t} \tilde{q} = 1 \equiv \frac{\partial}{\partial \tilde{p}} \tilde{H}, \tag{49}$$

$$\frac{\mathrm{d}}{\mathrm{d}t} \tilde{p} = -\frac{\varphi_0(\tilde{q}) - u_1}{\Delta x} \varphi_0'(\tilde{q}) - \frac{\varphi_1(\tilde{q}) - u_N}{\Delta x} \varphi_1'(\tilde{q}) \equiv -\frac{\partial}{\partial \tilde{q}} \tilde{H},$$

with initial conditions given by (see (40))

$$\mathbf{q}(0) = \psi_0(\mathbf{x}), \quad \mathbf{p}(0) = \psi_1(\mathbf{x}), \quad \tilde{q}(0) = \tilde{p}(0) = 0. \tag{50}$$

The first three equations in (49) exactly coincide with (46) (considering that $\tilde{q} \equiv t$), whereas the last one allows for the conservation of $\tilde{H}$:

$$\tilde{H}(\mathbf{q}(t), \mathbf{p}(t), \tilde{q}(t), \tilde{p}(t)) = \tilde{H}(\mathbf{q}(0), \mathbf{p}(0), 0, 0) \equiv H(\mathbf{q}(0), \mathbf{p}(0), 0), \quad t \geq 0.$$

Indeed, one readily sees that

$$\frac{\mathrm{d}}{\mathrm{d}t} \tilde{H}(\mathbf{q}, \mathbf{p}, \tilde{q}, \tilde{p}) = \overbrace{\nabla_{\mathbf{q}} \tilde{H}^\top \dot{\mathbf{q}} + \nabla_{\mathbf{p}} \tilde{H}^\top \dot{\mathbf{p}}}^{=0} + \underbrace{\frac{\partial}{\partial \tilde{q}} \tilde{H} \frac{\mathrm{d}}{\mathrm{d}t} \tilde{q} + \frac{\partial}{\partial \tilde{p}} \tilde{H} \frac{\mathrm{d}}{\mathrm{d}t} \tilde{p}}_{=0} = 0, \tag{51}$$

by virtue of (49). Consequently, by recalling that $\tilde{q} \equiv t$, from (44) and (51) one obtains:

$$\frac{\mathrm{d}}{\mathrm{d}t} H(\mathbf{q}, \mathbf{p}, t) = \frac{\partial}{\partial t} H(\mathbf{q}, \mathbf{p}, t) = \left[\frac{\varphi_0(t) - u_1}{\Delta x} \varphi_0'(t) + \frac{\varphi_1(t) - u_N}{\Delta x} \varphi_1'(t) \right],$$

which is the discrete counterpart of (37), via the approximation (41) and taking into account the boundary conditions (43). Consequently, one obtains the following semi-discrete analogue of (38):

$$H(\mathbf{q}(h), \mathbf{p}(h), h) - H(\mathbf{q}(0), \mathbf{p}(0), 0) = \int_0^h \left[\frac{u_{N+1}(t) - u_N(t)}{\Delta x} \varphi_1'(t) - \frac{u_1(t) - u_0(t)}{\Delta x} \varphi_0'(t) \right] \mathrm{d}t. \tag{52}$$

Remark 2. It is clear that (52) is equivalent to keep constant $\tilde{H}(\mathbf{q}(t), \mathbf{p}(t), t, \tilde{p}(t))$ along the solution of (49). Consequently, by conserving the augmented Hamiltonian $\tilde{H}$, one obtains that H satisfies a prescribed variation in time which, in turn, is consistent with the corresponding continuous one.

In order to simplify the notation, let us set

$$\mathbf{y} = \begin{pmatrix} \mathbf{q} \\ \mathbf{p} \\ \tilde{q} \\ \tilde{p}, \end{pmatrix}, \quad \tilde{J}_N = \left(\begin{array}{cc|c} & \frac{1}{\Delta x} I_N & \\ -\frac{1}{\Delta x} I_N & & \\ \hline & & 1 \\ & -1 & \end{array} \right), \tag{53}$$

so that (49)–(50) can be rewritten as

$$\dot{\mathbf{y}} = \tilde{J}_N \nabla \tilde{H}(\mathbf{y}), \quad t > 0, \quad \mathbf{y}(0) = (\psi_0(\mathbf{x})^\top, \psi_1(\mathbf{x})^\top, 0, 0)^\top. \tag{54}$$

3.2. Full discretization

The full discretization of (53)–(54) follows similar steps as those seen in Section 2.2 for (22). Let us then expand the right-hand side in (54) as done in (24)–(25), and consider the polynomial approximation of degree s given by (28), by formally replacing H with $\tilde{H}$. In such a case, one obtains energy conservation, since (compare with (33))

$$\tilde{H}(\boldsymbol{\sigma}(h)) - \tilde{H}(\boldsymbol{\sigma}(0)) = h \int_0^1 \nabla\tilde{H}(\boldsymbol{\sigma}(\tau h))^\top \dot{\boldsymbol{\sigma}}(\tau h) \mathrm{d}\tau = h \int_0^1 \nabla\tilde{H}(\boldsymbol{\sigma}(\tau h))^\top \sum_{j=0}^{s-1} P_j(\tau)\gamma_j(\boldsymbol{\sigma}) \mathrm{d}\tau = h \sum_{j=0}^{s-1} \gamma_j(\boldsymbol{\sigma})^\top \tilde{J}_N^{-\top} \gamma_j(\boldsymbol{\sigma}) = 0,$$

since

$$\tilde{J}_N^{-\top} = \begin{pmatrix} & \Delta x I_N & \\ -\Delta x I_N & & \\ \hline & & & 1 \\ & & -1 & \end{pmatrix} \tag{55}$$

is skew-symmetric. Consequently, if one is able to exactly compute the integrals, by means of a quadrature rule based at $k \geq s$ Gaussian points, with k large enough, energy conservation is gained. This is the case, provided that $\tilde{H}$ is a polynomial, that is, $f \in \Pi_\nu$ and $\varphi_0, \varphi_1 \in \Pi_\rho$, and, moreover, k satisfies:

$$k \geq \frac{1}{2}\max\{\nu s, 2\rho + s - 1, \rho + 2s - 1\} \tag{56}$$

(we observe that, in case $\rho = 0$, such a bound reduces to the bound (32), obtained in the case of periodic boundary conditions). When $\tilde{H}$ is not a polynomial, by approximating the integrals by means of a Gaussian quadrature of order $2k$, one obtains, with arguments similar to those used in (29)–(30),

$$\gamma_j(\boldsymbol{\sigma}) = \int_0^1 \tilde{J}_N \nabla\tilde{H}(\boldsymbol{\sigma}(\tau h)) P_j(\tau) \mathrm{d}\tau = \underbrace{\sum_{\ell=1}^k b_\ell P_j(c_\ell) \tilde{J}_N \nabla\tilde{H}(\boldsymbol{\sigma}(c_\ell h))}_{=\hat{\gamma}_j(\boldsymbol{\sigma})} + \Delta_j(h) \equiv \hat{\gamma}_j(\boldsymbol{\sigma}) + \Delta_j(h),$$

with

$$\Delta_j(h) = O(h^{2k-j}) \in \mathbb{R}^{2N+2}, \quad j = 0, \ldots, s-1. \tag{57}$$

In such a case, we have again a different polynomial $\mathbf{u} \in \Pi_s$, in place of $\boldsymbol{\sigma}$, solution of a problem formally still given by (31) with J_N and H replaced by $\tilde{J}_N$ and $\tilde{H}$, respectively. As a consequence, by taking into account (57), the error in the Hamiltonian $\tilde{H}$, at $t = h$, is given by (see (53)):

$$\tilde{H}(\mathbf{u}(h)) - \tilde{H}(\mathbf{u}(0)) = h \int_0^1 \nabla\tilde{H}(\mathbf{u}(\tau h))^\top \dot{\mathbf{u}}(\tau h) \mathrm{d}\tau = h \int_0^1 \nabla\tilde{H}(\mathbf{u}(\tau h))^\top \sum_{j=0}^{s-1} P_j(\tau)(\gamma_j(\mathbf{u}) - \Delta_j(h)) \mathrm{d}\tau$$

$$= h \sum_{j=0}^{s-1} \left[\overbrace{\gamma_j(\mathbf{u})^\top \tilde{J}_N^{-\top} \gamma_j(\mathbf{u})}^{=0} - \gamma_j(\mathbf{u})^\top \tilde{J}_N^{-\top} \Delta_j(h) \right] = h \underbrace{\Delta x \cdot N}_{<1} \cdot O(h^{2k}) \equiv O(h^{2k+1}),$$

where the last equality follows from (39), (55), and Lemma 1. Consequently, choosing k large enough allows us to approximate the Hamiltonian $\tilde{H}$ within full machine accuracy.

All the above arguments can be summarized by the following theorem, which generalizes Theorem 2 to the present case.

Theorem 3. *Assume $k \geq s$, and define $\mathbf{y}_1 = \mathbf{u}(h)$ as the new approximation to $\mathbf{y}(h)$, solution of (53)–(54), provided by a HBVM(k, s) method used with stepsize h. One then obtains:*

$$\mathbf{y}_1 - \mathbf{y}(h) = O(h^{2s+1}),$$

that is the method has order 2s. Moreover, assuming that f, φ_0, and φ_1 in (1) and (4) are suitably regular:

$$\tilde{H}(\mathbf{y}_1) - \tilde{H}(\mathbf{y}_0) = \begin{cases} 0, & \text{if } f \in \Pi_\nu, \varphi_0, \varphi_1 \in \Pi_\rho, \text{ and (56) holds true,} \\ O(h^{2k+1}), & \text{otherwise.} \end{cases}$$

Clearly, considerations similar to those stated in Remark 1 can be repeated also in the present situation.

Remark 3. In the case when $\varphi_0 = \varphi_1 \equiv 0$, we have $\tilde{p} \equiv 0$ and $\tilde{H} \equiv H$ (see (48)–(50)), therefore, as a consequence of Theorem 3 and Remark 1, we have (an at least practical) conservation of the original semi-discrete Hamiltonian.

As sketched at the beginning of this section, the conservation of the Hamiltonian, when the Dirichlet boundary conditions are homogeneous, may be exploited to show the well-posedness of the continuous problem, provided that the nonlinearity satisfies

suitable assumptions. Similarly, also in the discrete setting the stability of the solution follows from the conservation of the (semi-discrete) energy. As an example, if f is bounded from below (i.e. $f(u) \geq -L, L \geq 0, \forall u \in \mathbb{R}$), we have:

$$
\Delta x \|\mathbf{u}(t)\|^2 = \Delta x (\|\mathbf{p}(t)\|^2 + \|\mathbf{q}(t)\|^2) \leq \Delta x \left(\mathbf{p}(t)^\top \mathbf{p}(t) + \frac{\mathbf{q}(t)^\top T_N \mathbf{q}(t)}{\lambda_N} \right)
$$

$$
= \Delta x \left(\mathbf{p}(t)^\top \mathbf{p}(t) + \frac{\mathbf{q}(t)^\top T_N \mathbf{q}(t)}{\Delta x^2} \alpha^2 \right) \leq \Delta x \left(\mathbf{p}(t)^\top \mathbf{p}(t) + \frac{\mathbf{q}(t)^\top T_N \mathbf{q}(t)}{\Delta x^2} \right)
$$

$$
= 2(H(\mathbf{u}(t)) - \mathbf{e}^\top f(\mathbf{q}(t)) \Delta x) \leq 2(H(\mathbf{u}(0)) + L),
$$

where, for $N \gg 1$, $\lambda_N = 2[1 - \cos(\frac{\pi}{N+1})] \simeq (\pi \Delta x)^2$ is the minimum eigenvalue of T_N in (45) and $\alpha \simeq \pi^{-1}$.

Remark 4. Even in the case when the boundary conditions are non-homogeneous, conserving the augmented Hamiltonian $\tilde{H}$ may result in a more reliable reproduction of the original semi-discrete Hamiltonian H.

In particular, according to the analysis in [63], if the boundary conditions are small enough, we can assume that the variation on the Hamiltonian is quite small, that is $|\tilde{p}| \simeq \varepsilon \ll |\tilde{H}|$ and, therefore, the error on the semi-discrete Hamiltonian $H = \tilde{H} - \tilde{p}$ behaves as

$$
O(h^{2k}) + \varepsilon O(h^{2s}). \tag{58}
$$

Consequently, the error on H will approximately decrease with order $2k$, until $O(h^{2k}) \simeq \varepsilon O(h^{2s})$. This aspect will be confirmed by the numerical tests in Section 7.

4. The case of Neumann boundary conditions

As done in the case of Dirichlet boundary conditions, also when Neumann boundary conditions are prescribed, one starts from the formulation (36) of the continuous Hamiltonian function, and then considers its semi-discretization (42). In so doing, one arrives at the very same formulation (44), with T_N defined as in (45), whereas, by considering the Neumann boundary conditions (5), and the approximations (41) used to derive (42), $\boldsymbol{\varphi}(t)$ is now formally defined as follows:

$$
\boldsymbol{\varphi}(t) = (u_1 - \phi_0(t) \Delta x, \quad 0, \ldots, 0, \quad u_N + \phi_1(t) \Delta x)^\top.
$$

In fact, this is equivalent to use the following definitions for $u_0(t)$ and $u_{N+1}(t)$,

$$
u_0(t) = u_1 - \phi_0(t) \Delta x, \quad u_{N+1}(t) = u_N + \phi_1(t) \Delta x, \tag{59}
$$

which we shall use in the sequel. We prefer, however, to derive the semi-discrete Hamiltonian by following a slightly different route, as described below. In more details, starting from (42), one obtains:

$$
H = \Delta x \sum_{i=1}^{N} \left(\frac{1}{2} v_i^2 - u_i \frac{u_{i-1} - 2u_i + u_{i+1}}{2\Delta x^2} + f(u_i) \right) + \frac{1}{2} \left[u_{N+1} \frac{u_{N+1} - u_N}{\Delta x} - u_0 \frac{u_1 - u_0}{\Delta x} \right]
$$

$$
= \Delta x \sum_{i=2}^{N-1} \left(\frac{1}{2} v_i^2 - u_i \frac{u_{i-1} - 2u_i + u_{i+1}}{2\Delta x^2} + f(u_i) \right) + \frac{1}{2} \left[u_{N+1} \frac{u_{N+1} - u_N}{\Delta x} - u_0 \frac{u_1 - u_0}{\Delta x} \right]
$$

$$
+ \Delta x \left(\frac{1}{2} v_1^2 - u_1 \frac{u_0 - 2u_1 + u_2}{2\Delta x^2} + f(u_1) + \frac{1}{2} v_N^2 - u_N \frac{u_{N-1} - 2u_N + u_{N+1}}{2\Delta x^2} + f(u_N) \right)
$$

$$
= \Delta x \sum_{i=2}^{N-1} \left(\frac{1}{2} v_i^2 - u_i \frac{u_{i-1} - 2u_i + u_{i+1}}{2\Delta x^2} + f(u_i) \right) + \frac{1}{2} \left[\frac{(u_{N+1} - u_N)^2}{\Delta x} + \frac{(u_1 - u_0)^2}{\Delta x} \right]
$$

$$
+ \Delta x \left(\frac{1}{2} v_1^2 - u_1 \frac{-u_1 + u_2}{2\Delta x^2} + f(u_1) + \frac{1}{2} v_N^2 - u_N \frac{u_{N-1} - u_N}{2\Delta x^2} + f(u_N) \right),
$$

which can be cast in vector form as

$$
H \equiv H(\mathbf{q}, \mathbf{p}, t) = \Delta x \left[\frac{\mathbf{p}^\top \mathbf{p}}{2} + \frac{\mathbf{q}^\top T_N \mathbf{q}}{2\Delta x^2} + \mathbf{e}^\top f(\mathbf{q}) \right] + \frac{\mathbf{w}(\mathbf{q}, t)^\top \mathbf{w}(\mathbf{q}, t)}{2\Delta x}, \tag{60}
$$

where $\mathbf{e}$ has been defined in (21), $\mathbf{q}$ and $\mathbf{p}$ are defined at (40), whereas:

$$
T_N = \begin{pmatrix} 1 & -1 & & & \\ -1 & 2 & \ddots & & \\ & \ddots & \ddots & \ddots & \\ & & \ddots & 2 & -1 \\ & & & -1 & 1 \end{pmatrix} \in \mathbb{R}^{N \times N}, \quad \mathbf{w}(\mathbf{q}, t) = \begin{pmatrix} u_1 - u_0(t) \\ 0 \\ \vdots \\ 0 \\ u_{N+1}(t) - u_N \end{pmatrix} \in \mathbb{R}^N. \tag{61}
$$

We emphasize that $u_0(t)$ and $u_{N+1}(t)$ have to be regarded as known functions. Thus, with reference to (60)–(61), the corresponding semi-discrete Hamiltonian problem is given by:

$$\dot{\mathbf{q}} = \mathbf{p} \equiv \frac{1}{\Delta x}\nabla_{\mathbf{p}} H, \quad t > 0,$$
$$\dot{\mathbf{p}} = -\frac{1}{\Delta x^2} T_N \mathbf{q} + \frac{\Sigma}{\Delta x^2} \mathbf{w}(\mathbf{q}, t) - f'(\mathbf{q}) \equiv -\frac{1}{\Delta x}\nabla_{\mathbf{q}} H, \tag{62}$$

where

$$\Sigma = \begin{pmatrix} -1 & & & & \\ & 0 & & & \\ & & \ddots & & \\ & & & 0 & \\ & & & & 1 \end{pmatrix} \in \mathbb{R}^{N \times N}.$$

By considering (59), one has then

$$\frac{\Sigma}{\Delta x^2}\mathbf{w}(\mathbf{q}, t) = \frac{1}{\Delta x^2}\begin{pmatrix} u_0 - u_1 \\ 0 \\ \vdots \\ 0 \\ u_{N+1} - u_N \end{pmatrix} = \frac{1}{\Delta x}\begin{pmatrix} -\phi_0(t) \\ 0 \\ \vdots \\ 0 \\ \phi_1(t) \end{pmatrix} \equiv \frac{1}{\Delta x}\boldsymbol{\phi}(t),$$

thus obtaining the final shape of (62):

$$\dot{\mathbf{q}} = \mathbf{p}, \quad t > 0, \tag{63}$$
$$\dot{\mathbf{p}} = -\frac{1}{\Delta x^2} T_N \mathbf{q} + \frac{1}{\Delta x}\boldsymbol{\phi}(t) - f'(\mathbf{q}).$$

As in the case of Dirichlet boundary conditions, problem (63) is Hamiltonian with the non-autonomous Hamiltonian (60): again, we can transform this latter into an autonomous one, by introducing the couple of auxiliary conjugate variables (47) and the augmented Hamiltonian (compare with (48))

$$\tilde{H}(\mathbf{q}, \mathbf{p}, \tilde{q}, \tilde{p}) = H(\mathbf{q}, \mathbf{p}, \tilde{q}) + \tilde{p}, \tag{64}$$

with H now given by (60). The dynamical system corresponding to this new Hamiltonian function is, for $t > 0$:

$$\dot{\mathbf{q}} = \mathbf{p} \equiv \frac{1}{\Delta x}\nabla_{\mathbf{p}}\tilde{H},$$
$$\dot{\mathbf{p}} = -\frac{1}{\Delta x^2} T_N \mathbf{q} + \frac{1}{\Delta x}\boldsymbol{\phi} - f'(\mathbf{q}) \equiv -\frac{1}{\Delta x}\nabla_{\mathbf{q}}\tilde{H},$$
$$\frac{d}{dt}\tilde{q} = 1 \equiv \frac{\partial}{\partial\tilde{p}}\tilde{H}, \tag{65}$$
$$\frac{d}{dt}\tilde{p} = -\frac{\partial}{\partial\tilde{q}}\tilde{H},$$

with initial conditions as in (50). Concerning the last equation in (65), from (64), (60)–(61), and (59), one has, by considering that $q_i(t) \equiv u_i(t), q_i'(t) = p_i(t) \equiv v_i(t)$ (see (40)), and $\tilde{q} \equiv t$,

$$\frac{d}{dt}\tilde{p} = -\frac{\partial}{\partial\tilde{q}}\tilde{H} = -\frac{1}{\Delta x}((u_0(\tilde{q}) - u_1)v_0(\tilde{q}) + (u_{N+1}(\tilde{q}) - u_N)v_{N+1}(\tilde{q}))$$
$$= \phi_0(\tilde{q})[v_1 - \Delta x\phi_0'(\tilde{q})] - \phi_1(\tilde{q})[v_N + \Delta x\phi_1'(\tilde{q})]. \tag{66}$$

Now, problem (65)–(66) is Hamiltonian with an autonomous Hamiltonian function, so that its energy (64) is conserved (clearly, considerations similar to those reported in Remark 2 for the Dirichlet case can be now repeated).

Also now, the discrete problem can be cast in vector form, formally as done in (53)–(54). Moreover, concerning the discretization issue, arguments similar to those seen in Section 3.2 apply to the present case. In particular, the following result holds true, the proof being similar to that of Theorems 2 and 3.

Theorem 4. *Let* $\mathbf{y}_1 = \mathbf{u}(h)$ *be the approximation to* $\mathbf{y}(h)$, *solution of (53)–(54), formally equivalent to (65)–(66), provided by a HBVM(k, s) method used with stepsize h. One then obtains:*

$$\mathbf{y}_1 - \mathbf{y}(h) = O(h^{2s+1}),$$

that is the method has order 2s. Moreover, assuming that f, ϕ_0, and ϕ_1 in (1) and (5) are suitably regular:

$$\tilde{H}(\mathbf{y}_1) - \tilde{H}(\mathbf{y}_0) = \begin{cases} 0, & \text{if } f \in \Pi_\nu, \phi_0, \phi_1 \in \Pi_\rho, \text{ with} \\ & 2k \geq \max\{\nu s, 2\rho + s - 1, 2s + \rho\}, \\ O(h^{2k+1}), & \text{otherwise.} \end{cases}$$

Evidently, considerations similar to those stated in Remarks 1 and 4 can be repeated also in the present situation.

5. Periodic boundary conditions revisited

The case of periodic boundary conditions, i.e. (1)–(2), deserves to be further investigated. In fact, the finite-difference discretizations considered above, turn out to provide a second-order spatial accuracy, in the used stepsize Δx. When either Dirichlet or Neumann boundary conditions are specified, it is not possible to easily derive higher-order semi-discrete Hamiltonian formulations of the problem. Conversely, in the case of periodic boundary conditions, this can be easily accomplished. As a matter of fact, by suitably replacing the circulant matrix T_N defined in (20), one obtains that the Hamiltonian (19) remains formally the same, as well as the semi-discrete Hamiltonian problem (17). For this purpose, any symmetric high-order approximation to the second spatial derivative could be used (see e.g., [2]), to derive a new circulant and symmetric band-matrix. As an example, the following matrix provides a fourth-order spatial approximation [76],

$$T_N = - \begin{pmatrix} -\frac{5}{2} & \frac{4}{3} & -\frac{1}{12} & & & -\frac{1}{12} & \frac{4}{3} \\ \frac{4}{3} & \ddots & \ddots & \ddots & & & -\frac{1}{12} \\ -\frac{1}{12} & & \ddots & \ddots & \ddots & \ddots & \\ & & \ddots & \ddots & \ddots & \ddots & \ddots \\ & & & \ddots & \ddots & \ddots & \ddots & -\frac{1}{12} \\ -\frac{1}{12} & & & & \ddots & \ddots & \ddots & \frac{4}{3} \\ \frac{4}{3} & -\frac{1}{12} & & & -\frac{1}{12} & \frac{4}{3} & -\frac{5}{2} \end{pmatrix} \in \mathbb{R}^{N \times N}, \tag{67}$$

whereas, the following one provides a sixth-order spatial approximation (see [2] for additional examples):

$$T_N = - \begin{pmatrix} -\frac{49}{18} & \frac{3}{2} & -\frac{3}{20} & \frac{1}{90} & & \frac{1}{90} & -\frac{3}{20} & \frac{3}{2} \\ \frac{3}{2} & \ddots & \ddots & \ddots & \ddots & & \frac{1}{90} & -\frac{3}{20} \\ -\frac{3}{20} & & \ddots & \ddots & \ddots & \ddots & \ddots & \frac{1}{90} \\ \frac{1}{90} & & \ddots & \ddots & \ddots & \ddots & \ddots & \ddots \\ & & \ddots & \ddots & \ddots & \ddots & \ddots & \ddots & \frac{1}{90} \\ \frac{1}{90} & & \ddots & \ddots & \ddots & \ddots & \ddots & -\frac{3}{20} \\ -\frac{3}{20} & \frac{1}{90} & & & \ddots & \ddots & \ddots & \ddots & \frac{3}{2} \\ \frac{3}{2} & -\frac{3}{20} & \frac{1}{90} & & \frac{1}{90} & -\frac{3}{20} & \frac{3}{2} & -\frac{49}{18} \end{pmatrix} \in \mathbb{R}^{N \times N}. \tag{68}$$

5.1. Fourier space discretization

An alternative approach, which we shall investigate in the sequel, is that of using a Fourier approximation in space (see, e.g., [37]). For this purpose, let us consider the following complete set of orthonormal functions in [0, 1]:

$$c_0(x) \equiv 1, \quad c_k(x) = \sqrt{2}\cos(2k\pi x), \quad s_k(x) = \sqrt{2}\sin(2k\pi x), \quad k = 1, 2, \ldots, \tag{69}$$

so that

$$\int_0^1 c_i(x)c_j(x)\,dx = \int_0^1 s_i(x)s_j(x)\,dx = \delta_{ij}, \quad \int_0^1 c_i(x)s_j(x)\,dx = 0, \quad \forall i, j. \tag{70}$$

The following expansion of the solution of (1)–(2) is a slightly different way of writing the usual Fourier expansion in space:

$$u(x, t) = c_0(x)\gamma_0(t) + \sum_{n \geq 1} [c_n(x)\gamma_n(t) + s_n(x)\eta_n(t)]$$

$$\equiv \gamma_0(t) + \sum_{n \geq 1} [c_n(x)\gamma_n(t) + s_n(x)\eta_n(t)], \quad x \in [0, 1], \quad t \geq 0, \tag{71}$$

with

$$\gamma_n(t) = \int_0^1 c_n(x)u(x,t)dx, \quad \eta_n(t) = \int_0^1 s_n(x)u(x,t)dx,$$

which is allowed because of the periodic boundary conditions (2). Consequently, by taking into account (70), the first equation in (1) can be rewritten as:

$$\ddot{\gamma}_n(t) = -(2\pi n)^2\gamma_n(t) - \int_0^1 c_n(x)f'\left(\gamma_0(t) + \sum_{j\geq 1}[c_j(x)\gamma_j(t) + s_j(x)\eta_j(t)]\right)dx, \quad n \geq 0,$$

$$\ddot{\eta}_n(t) = -(2\pi n)^2\eta_n(t) - \int_0^1 s_n(x)f'\left(\gamma_0(t) + \sum_{j\geq 1}[c_j(x)\gamma_j(t) + s_j(x)\eta_j(t)]\right)dx, \quad n \geq 1,$$

(72)

where the double dot denotes, as usual, the second time derivative. The initial conditions are clearly given by (see (1)):

$$\gamma_n(0) = \int_0^1 c_n(x)\psi_0(x)dx, \qquad \eta_n(0) = \int_0^1 s_n(x)\psi_0(x)dx,$$

$$\dot{\gamma}_n(0) = \int_0^1 c_n(x)\psi_1(x)dx, \qquad \dot{\eta}_n(0) = \int_0^1 s_n(x)\psi_1(x)dx.$$

(73)

By introducing the infinite vectors

$$\boldsymbol{\omega}(x) = (c_0(x), \quad c_1(x), \quad s_1(x), \quad c_2(x), \quad s_2(x), \quad \ldots)^\top,$$

$$\mathbf{q}(t) = (\gamma_0(t), \quad \gamma_1(t), \quad \eta_1(t), \quad \gamma_2(t), \quad \eta_2(t), \quad \ldots)^\top,$$

(74)

the infinite matrix

$$D = \begin{pmatrix} 0 & & & & & \\ & (2\pi)^2 & & & & \\ & & (2\pi)^2 & & & \\ & & & (4\pi)^2 & & \\ & & & & (4\pi)^2 & \\ & & & & & \ddots \end{pmatrix},$$

(75)

and considering that (see (71))

$$u(x,t) = \boldsymbol{\omega}(x)^\top\mathbf{q}(t),$$

(76)

problem (72) can be cast in vector form as:

$$\dot{\mathbf{q}}(t) = \mathbf{p}(t), \quad t > 0,$$

$$\dot{\mathbf{p}}(t) = -D\mathbf{q}(t) - \int_0^1 \boldsymbol{\omega}(x)f'(\boldsymbol{\omega}(x)^\top\mathbf{q}(t))dx,$$

(77)

with the initial conditions (73) written, more compactly, as

$$\mathbf{q}(0) = \int_0^1 \boldsymbol{\omega}(x)\psi_0(x)dx, \quad \mathbf{p}(0) = \int_0^1 \boldsymbol{\omega}(x)\psi_1(x)dx.$$

(78)

The following result then holds true.

Theorem 5. *Problem (77) is Hamiltonian, with Hamiltonian*

$$H(\mathbf{q}, \mathbf{p}) = \frac{1}{2}\mathbf{p}^\top\mathbf{p} + \frac{1}{2}\mathbf{q}^\top D\mathbf{q} + \int_0^1 f(\boldsymbol{\omega}(x)^\top\mathbf{q})dx.$$

(79)

This latter is equivalent to the Hamiltonian (7), via the expansion (71)–(76).

Proof. The first statement is straightforward, by considering that

$$\nabla_\mathbf{q}f(\boldsymbol{\omega}(x)^\top\mathbf{q})) = f'(\boldsymbol{\omega}(x)^\top\mathbf{q})\boldsymbol{\omega}(x).$$

The second statement then easily follows, by taking into account (76), from the fact that, see (6), (70), (71), and (74):

$$\int_0^1 v(x,t)^2dx = \int_0^1 u_t(x,t)^2dx = \int_0^1 \left(\dot{\gamma}_0(t) + \sum_{n\geq 1}[\dot{\gamma}_n(t)c_n(x) + \dot{\eta}_n(t)s_n(x)]\right)^2 dx$$

$$= \dot{\gamma}_0(t)^2 + \sum_{n\geq 1}[\dot{\gamma}_n(t)^2 + \dot{\eta}_n(t)^2] \equiv \mathbf{p}(t)^\top\mathbf{p}(t),$$

and

$$\int_0^1 u_x(x,t)^2 dx = \int_0^1 \left(\sum_{n \geq 1} 2\pi n [\eta_n(t)c_n(x) - \gamma_n(t)s_n(x)] \right)^2 dx = \sum_{n \geq 1} (2\pi n)^2 [\eta_n(t)^2 + \gamma_n(t)^2] = \mathbf{q}(t)^\top D \mathbf{q}(t).$$

□

5.2. Truncated Fourier–Galerkin approximation

In order to obtain a practical computational procedure, one usually truncates the infinite expansion (71) to a finite sum:

$$u(x,t) \approx \gamma_0(t) + \sum_{n=1}^N [c_n(x)\gamma_n(t) + s_n(x)\eta_n(t)] \equiv u_N(x,t), \tag{80}$$

which converges more than exponentially with N to u, if this latter is an analytical function.[4] In other words, we look for an approximation to $u(x,t)$ belonging to the functional subspace (see (69))

$$\mathcal{V}_N = \text{span}\{c_0(x), c_1(x), \ldots, c_N(x), s_1(x), \ldots, s_N(x)\}.$$

Clearly, such a truncated expansion will not satisfy problem (1)–(2). Nevertheless, in the spirit of Fourier–Galerkin methods [5], by requiring that the residual

$$R(u_N) := (u_N)_{tt} - (u_N)_{xx} + f'(u_N)$$

be orthogonal to $\mathcal{V}_N$, one obtains the *weak formulation* of problem (1)–(2), consisting in the following set of $2N+1$ differential equations,

$$\ddot{\gamma}_n(t) = -(2\pi n)^2 \gamma_n(t) - \int_0^1 c_n(x) f' \left(\gamma_0(t) + \sum_{j=1}^N \left[c_j(x)\gamma_j(t) + s_j(x)\eta_j(t) \right] \right) dx, \quad n = 0, \ldots, N,$$

$$\ddot{\eta}_n(t) = -(2\pi n)^2 \eta_n(t) - \int_0^1 s_n(x) f' \left(\gamma_0(t) + \sum_{j=1}^N [c_j(x)\gamma_j(t) + s_j(x)\eta_j(t)] \right) dx, \quad n = 1, \ldots, N, \tag{81}$$

approximating the leading ones in (72). By defining the finite vectors in $\mathbb{R}^{2N+1}$ (compare with (74)),

$$\boldsymbol{\omega}_N(x) = (c_0(x), \quad c_1(x), \quad s_1(x), \quad c_2(x), \quad s_2(x), \quad \ldots, \quad c_N(x), s_N(x))^\top,$$

$$\mathbf{q}_N(t) = (\gamma_0(t), \quad \gamma_1(t), \quad \eta_1(t), \quad \gamma_2(t), \quad \eta_2(t), \quad \ldots, \quad \gamma_N(t), \quad \eta_N(t))^\top,$$

the matrix (compare with (75))

$$D_N = \begin{pmatrix} 0 & & & & & & \\ & (2\pi)^2 & & & & & \\ & & (2\pi)^2 & & & & \\ & & & (4\pi)^2 & & & \\ & & & & (4\pi)^2 & & \\ & & & & & \ddots & \\ & & & & & & (2N\pi)^2 \\ & & & & & & & (2N\pi)^2 \end{pmatrix} \in \mathbb{R}^{(2N+1) \times (2N+1)}, \tag{82}$$

and considering that (compare with (80))

$$u_N(x,t) = \boldsymbol{\omega}_N(x)^\top \mathbf{q}_N(t), \tag{83}$$

the Eqs. (81), which have to be satisfied by (83), can be cast in vector form as:

$$\dot{\mathbf{q}}_N(t) = \mathbf{p}_N(t), \quad t > 0,$$

$$\dot{\mathbf{p}}_N(t) = -D_N \mathbf{q}_N(t) - \int_0^1 \boldsymbol{\omega}_N(x) f'(\boldsymbol{\omega}_N(x)^\top \mathbf{q}_N(t)) dx, \tag{84}$$

for a total of $4N+2$ differential equations. Clearly, from (73) one obtains that the initial conditions for (84) are given by:

$$\mathbf{q}_N(0) = \int_0^1 \boldsymbol{\omega}_N(x) \psi_0(x) dx, \quad \mathbf{p}_N(0) = \int_0^1 \boldsymbol{\omega}_N(x) \psi_1(x) dx. \tag{85}$$

---

[4] We refer, e.g., to [27], for a corresponding comprehensive error analysis.

The following result then easily follows by means of arguments similar to those used to prove Theorem 5.

Theorem 6. *Problem (84) is Hamiltonian, with Hamiltonian*

$$H_N(\mathbf{q}_N, \mathbf{p}_N) = \frac{1}{2}\mathbf{p}_N^\top \mathbf{p}_N + \frac{1}{2}\mathbf{q}_N^\top D_N \mathbf{q}_N + \int_0^1 f(\boldsymbol{\omega}_N(x)^\top \mathbf{q}_N)\mathrm{d}x. \tag{86}$$

We observe that (86) is equivalent to a truncated Fourier expansion of the Hamiltonian (7) (see also (79)). Moreover, it is worth mentioning that using the initial conditions (85), in place of (78), results in an error e_N, in the initial data, given by

$$e_N^2 = \int_0^1 (\psi_0(x) - \boldsymbol{\omega}_N(x)^\top \mathbf{q}_N(0))^2 \mathrm{d}x + \int_0^1 (\psi_1(x) - \boldsymbol{\omega}_N(x)^\top \mathbf{p}_N(0))^2 \mathrm{d}x$$

$$= \sum_{n>N}\left[\int_0^1 c_n(x)\psi_0(x)\mathrm{d}x\right]^2 + \left[\int_0^1 s_n(x)\psi_0(x)\mathrm{d}x\right]^2 + \sum_{n>N}\left[\int_0^1 c_n(x)\psi_1(x)\mathrm{d}x\right]^2 + \left[\int_0^1 s_n(x)\psi_1(x)\mathrm{d}x\right]^2. \tag{87}$$

However, it must be stressed that, unlike the finite-difference case, both e_N and the approximation (86) to the continuous Hamiltonian, converge more than exponentially in N (e_N to 0, and H_N to H), provided that the involved functions are analytical.

5.3. Full discretization

Since problem (84) is Hamiltonian, with an autonomous Hamiltonian, this latter is conserved along the solution. Consequently, energy conserving methods can be conveniently used for its solution. In particular, Theorem 2 continues formally to hold for HBVM(k, s) methods. However, the integral appearing in (84) need to be, in turn, approximated by means of a suitable quadrature rule. For this purpose, it could be convenient to do this by means of a composite trapezoidal rule, due to the fact that the argument is a periodic function. Consequently, having set

$$\mathbf{g}_N(x, t) = \boldsymbol{\omega}_N(x) f'(\boldsymbol{\omega}_N(x)^\top \mathbf{q}_N(t)), \tag{88}$$

the uniform mesh on [0, 1]

$$x_i = i\Delta x, \quad i = 0, \ldots, m, \quad \Delta x = \frac{1}{m}, \tag{89}$$

and considering that $\mathbf{g}_N(0, t) = \mathbf{g}_N(1, t)$, one obtains:

$$\int_0^1 \mathbf{g}_N(x, t)\mathrm{d}x = \Delta x \sum_{i=1}^m \frac{\mathbf{g}_N(x_{i-1}, t) + \mathbf{g}_N(x_i, t)}{2} + R(m) = \frac{1}{m}\sum_{i=0}^{m-1} \mathbf{g}_N(x_i, t) + R(m). \tag{90}$$

Let us study the error $R(m)$. For this purpose, we need some preliminary result.

Lemma 2. *Let us consider the trigonometric polynomial*

$$p(x) = \sum_{k=0}^K [a_k \cos(2k\pi x) + b_k \sin(2k\pi x)], \tag{91}$$

and the uniform mesh (89). Then, for all $m \geq K + 1$, one obtains:

$$\int_0^1 p(x)\mathrm{d}x = \frac{1}{m}\sum_{i=0}^{m-1} p(x_i).$$

Proof. See, e.g., [34, Th 5.1.4]. □

Lemma 3. *Let us consider the trigonometric polynomial (91) and the uniform mesh (89). Then, for all $m \geq N + K + 1$, one obtains:*

$$\int_0^1 \cos(2j\pi x)p(x)\mathrm{d}x = \frac{1}{m}\sum_{i=0}^{m-1} \cos(2j\pi x_i)p(x_i), \tag{92}$$

$$\int_0^1 \sin(2j\pi x)p(x)\mathrm{d}x = \frac{1}{m}\sum_{i=0}^{m-1} \sin(2j\pi x_i)p(x_i), \quad j = 0, \ldots, N. \tag{93}$$

Proof. By virtue of the prosthaphaeresis formulae, one has, for all $j = 0, \ldots, N$ and $k = 0, \ldots, K$:

$$\cos(2j\pi x)\cos(2k\pi x) = \frac{1}{2}[\cos(2(k+j)\pi x) + \cos(2(k-j)\pi x)],$$

$$\cos(2j\pi x)\sin(2k\pi x) = \frac{1}{2}[\sin(2(k+j)\pi x) + \sin(2(k-j)\pi x)],$$

$$\sin(2j\pi x)\cos(2k\pi x) = \frac{1}{2}[\sin(2(k+j)\pi x) - \sin(2(k-j)\pi x)],$$

$$\sin(2j\pi x)\sin(2k\pi x) = \frac{1}{2}[\cos(2(k-j)\pi x) - \cos(2(k+j)\pi x)].$$

Consequently, the integrals at the left-hand side in (92)–(93) are trigonometric polynomials of degree at most $N + K$. By virtue of Lemma 2, it then follows that they are exactly computed by means of the composite trapezoidal rule at the corresponding right-hand sides, provided that $m \geq N + K + 1$. □

By virtue of Lemma 3, the following result follows at once.

Theorem 7. *Let the function f appearing in (88) (see also (83)) be a polynomial of degree ν, and let us consider the uniform mesh (89). Then, with reference to (90), for all $m \geq \nu N + 1$ one obtains:*

$$R(m) = 0 \quad i.e., \quad \int_0^1 \mathbf{g}_N(x,t)\mathrm{d}x = \frac{1}{m}\sum_{i=0}^{m-1}\mathbf{g}_N(x_i,t).$$

For a general function f, the following result holds true.

Theorem 8. *Let the function $\mathbf{g}_N(x,t)$ defined at (88), with t a fixed parameter, belong to $W_{per}^{r,p}$, the Banach space of periodic functions on $\mathbb{R}$ whose distribution derivatives up to order r belong to $L_{per}^p(\mathbb{R})$. Then, with reference to (89)–(90), one has:*

$$R(m) = O(m^{-r}).$$

Proof. See [60, Th. 1.1]. □

We end this section by mentioning that different approaches could be also used for approximating the integral appearing in (84): we refer, e.g., to [35], for a comprehensive review on this topic.

6. Implementation of the methods

The efficient implementation of HBVMs has been studied in [12,13,18]. We here sketch the application of a HBVM(k,s) method for solving (17), since the application to (49), (65), and (84) is similar. We consider the very first application of the method, so that the index of the time-step can be skipped. As remarked in [18], the discrete problem generated by a HBVM(k,s) method is more conveniently recast in terms of the s coefficients of the polynomial (31), instead of the k stages of the Runge–Kutta formulation (35). Moreover, since in the case of the semi-discrete formulation of the wave equation the Hamiltonian is separable, additional savings are possible, since the dimension of the problem can be halved, as we are going to sketch.[5] Let us then split the stage vector Y of the Runge–Kutta formulation, into Q and P, corresponding to the stages for $\mathbf{q}$ and $\mathbf{p}$, respectively. Consequently, from (35) and (17)–(18), one obtains, by setting $\mathbf{q}_0 = \mathbf{q}(0)$, $\mathbf{p}_0 = \mathbf{p}(0)$, and h the time-step:

$$Q = \mathbf{e}\otimes\mathbf{q}_0 + h\mathcal{IP}^\top\Omega\otimes I_N P, \quad P = \mathbf{e}\otimes\mathbf{p}_0 - h\mathcal{IP}^\top\Omega\otimes I_N F(Q), \tag{94}$$

where (see (17) and (20))

$$F(Q) = \frac{1}{\Delta x^2}I_k\otimes T_N Q + f'(Q), \tag{95}$$

with an obvious meaning of $f'(Q)$. By considering the following properties of the matrices $\mathcal{P}$ and $\mathcal{I}$, due to corresponding properties of Legendre polynomials [18],

- $\mathcal{IP}^\top\Omega\mathbf{e} = \mathbf{c}$,

- $\mathcal{P}^\top\Omega\mathcal{I} = X_s \equiv \begin{pmatrix} \frac{1}{2} & -\xi_1 & & \\ \xi_1 & 0 & \ddots & \\ & \ddots & \ddots & -\xi_{s-1} \\ & & \xi_{s-1} & 0 \end{pmatrix}$,

  with

  $$\xi_i = \left(2\sqrt{4i^2-1}\right)^{-1}, \quad i = 1,\ldots,s-1, \tag{96}$$

  substitution of the latter equation in (94) in the former one gives:

$$Q = \mathbf{e}\otimes\mathbf{q}_0 + h\mathbf{c}\otimes\mathbf{p}_0 - h^2\mathcal{I}X_s\mathcal{P}^\top\Omega\otimes I_N F(Q).$$

---

[5] This is not the case when considering different Hamiltonian PDEs, such as, e.g., the nonlinear Schrödinger equation.

By setting[6]

$$\boldsymbol{\gamma} = \mathcal{P}^\top \Omega \otimes I_N F(Q) \equiv \begin{pmatrix} \gamma_0 \\ \vdots \\ \gamma_{s-1} \end{pmatrix},$$

one then obtains the following discrete problem (of block dimension s):

$$G(\boldsymbol{\gamma}) \equiv \boldsymbol{\gamma} - \mathcal{P}^\top \Omega \otimes I_N F(\mathbf{e} \otimes \mathbf{q}_0 + h\mathbf{c} \otimes \mathbf{p}_0 - h^2 \mathcal{I} X_s \otimes I_N \boldsymbol{\gamma}) = \mathbf{0}. \tag{97}$$

Once (97) is solved, the new approximations are then given by (see (96)) [18]:

$$\mathbf{p}_1 = \mathbf{p}_0 + h\gamma_0, \quad \mathbf{q}_1 = \mathbf{q}_0 + h\mathbf{p}_0 + h^2 \left(\frac{1}{2}\gamma_0 - \xi_1\gamma_1 \right).$$

Consequently, the solution of the discrete problem (97) is the bulk of the computational cost of the step. For its solution, one could use the following simplified Newton iteration,

$$\left(I_s \otimes I_N + \frac{h^2}{\Delta x^2} X_s^2 \otimes T_N \right) \Delta \boldsymbol{\gamma}^\ell = -G(\boldsymbol{\gamma}^\ell) \equiv \boldsymbol{\eta}^\ell, \quad \ell = 0, 1, \ldots, \tag{98}$$

which only considers the (main) linear part of the function F (see (95)). However, even though the coefficient matrix of such iteration is constant, nevertheless, it has dimension sN. To reduce the computational cost, it is then better to use a *blended iteration* [18] (see also [10,23,24]), formally defined as:

$$\boldsymbol{\eta}_1^\ell = \rho_s^2 X_s^{-2} \otimes I_N \boldsymbol{\eta}^\ell, \tag{99}$$

$$\Delta \boldsymbol{\gamma}^\ell = I_s \otimes M_N^{-1}[\boldsymbol{\eta}_1^\ell + I_s \otimes M_N^{-1}(\boldsymbol{\eta}^\ell - \boldsymbol{\eta}_1^\ell)], \quad \ell = 0, 1, \ldots, \tag{100}$$

where

$$\rho_s = \min_{\lambda \in \sigma(X_s)} |\lambda|, \quad M_N = I_N + \left(\frac{h\rho_s}{\Delta x} \right)^2 T_N,$$

with $\sigma(X_s)$ denoting the spectrum of matrix X_s. Consequently, the computational cost of each iteration is given by:

- The evaluation of $\boldsymbol{\eta}^\ell$ in (98). This requires k evaluations of the right-hand side of the second equation in (17) (see (95)–(98)) plus $(4ks + 3k + s)N$ *flops*.[7]
- The evaluation of $\boldsymbol{\eta}_1^\ell$ in (99). Concerning matrix $\rho_s^{-1} X_s$, one can either invert and square it in advance, so that the costs for computing $\boldsymbol{\eta}_1^\ell$ is $2s^2 N$ *flops*, or solve 2 tridiagonal linear systems, so that, once the factorization is computed,[8] the cost per iteration amounts to $10sN$ *flops*. Consequently, the corresponding computational cost is given by $2\min\{s, 5\}sN$ *flops*.
- The evaluation of $\Delta \boldsymbol{\gamma}^\ell$ in (100). This requires solution of $2s$ linear systems with the symmetric matrix M_N plus $2sN$ *flops*. Concerning matrix M_N, an additional saving of computational effort is gained by retaining only its tridiagonal part (or by considering an approximate inverse).[9] In such a case, after its factorization,[10] one has a cost of less than $10sN$ *flops*. The total cost is then less than $12sN$ *flops*.

In conclusion, the total cost per iteration amounts to k function evaluations plus $(13s + 3k + 2\min\{s, 5\}s + 4ks)N$ *flops*.

It is worth mentioning that the same complexity is obtained in the case of Dirichlet or Neumann boundary conditions, by considering the corresponding tridiagonal matrices (45) and (61), respectively. Instead, when using the Fourier–Galerkin spatial semi-discretization, one obtains that matrix M_N is given by

$$M_N = I_{2N+1} + (h\rho_s)^2 D_N \in \mathbb{R}^{(2N+1)\times(2N+1)},$$

where matrix D_N is *diagonal* (see (82)). Consequently, also M_N is a diagonal matrix and, therefore, the complexity per iteration, besides the functions evaluations of the second equation in (84) (which are the same as before i.e., k), decreases. As a matter of fact, the required *flops* per iteration are now given by the dimension of the problem, times a factor $(5s + 3k + 2\min\{s, 5\}s + 4ks)$, in place of the factor $(13s + 3k + 2\min\{s, 5\}s + 4ks)$ seen above.

As a result of the previous arguments, one then expects a complexity per step which is *linear* in the dimension of the problem and, therefore, comparable with that of an explicit method. Moreover, in contrast to the A-stable HBVM(k, s) methods, explicit methods may suffer from stepsize restrictions due to stability reasons, as we shall see in the numerical tests.

Remark 5. Of course, the global complexity will depend on the total number of nonlinear iterations. This aspect will be numerically investigated in the next section, where we report the total number of nonlinear iterations required by some HBVM(k, s) methods for solving a problem for the *sine-Gordon* equation with various time-steps.

---

[6] Here, γ_j is given by the entries of the vector $\hat{\gamma}_j(\mathbf{u})$ in (31) corresponding to the $\mathbf{q}$ components only. Consequently, it has a halved dimension, w.r.t. this latter vector.

[7] We count as 1 *flop*, one elementary *floating-point operation.

[8] This costs less than $3s$ *flops*.

[9] In general, the matrix becomes *banded*, when considering higher-order discretizations, see, e.g., (67)–(68).

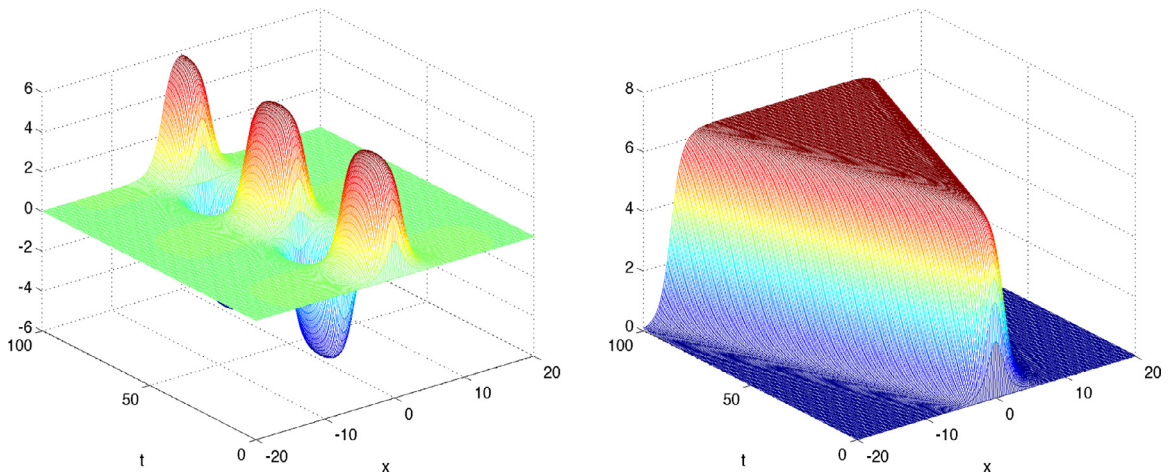[10] This costs less than $3N$ *flops*.

Fig. 1. *Breather* solution for $\gamma = 1.01$ (left plot), and *kink–antikink* solution for $\gamma = 0.99$ (right plot).
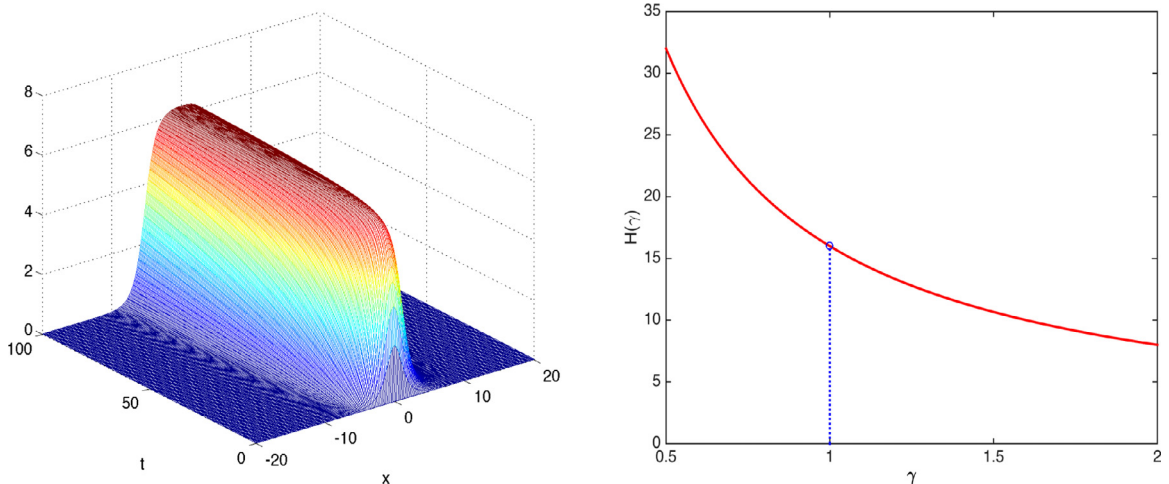

Fig. 2. *Double-pole* solution for $\gamma = 1$ (left plot), and Hamiltonian as a function of γ (right plot).

7. Numerical tests

We here consider a few numerical tests, concerning the so called *sine-Gordon* equation, which is in the form (1):

$$u_{tt}(x,t) = u_{xx}(x,t) - \sin(u(x,t)), \quad x \in [-20, 20], \quad t \geq 0. \tag{101}$$

In particular, we shall consider *soliton-like* solutions, as described in [83], defined by the initial conditions:

$$u(x,0) \equiv 0, \quad u_t(x,0) = \frac{4}{\gamma} \operatorname{sech}\left(\frac{x}{\gamma}\right), \quad \gamma > 0. \tag{102}$$

Depending on the value of the positive parameter γ, the solution is known to be given by:

$$u(x,t) = 4 \operatorname{atan}\left[\varphi(t;\gamma) \operatorname{sech}\left(\frac{x}{\gamma}\right)\right], \tag{103}$$

with

$$\varphi(t;\gamma) = \begin{cases} (\sqrt{\gamma^2 - 1})^{-1} \sin(\gamma^{-1}\sqrt{\gamma^2 - 1}\,t), & \text{if} \quad \gamma > 1, \\ t, & \text{if} \quad \gamma = 1, \\ (\sqrt{1 - \gamma^2})^{-1} \sinh(\gamma^{-1}\sqrt{1 - \gamma^2}\,t), & \text{if} \quad 0 < \gamma < 1. \end{cases}$$

The three cases are shown in Figs. 1 and 2: on the left of Fig. 1 is the plot of the first soliton (obtained for $\gamma > 1$), which is named *breather*; on the right plot of Fig. 1 is the case $0 < \gamma < 1$, which is named *kink–antikink*; at last, the case $\gamma = 1$, which
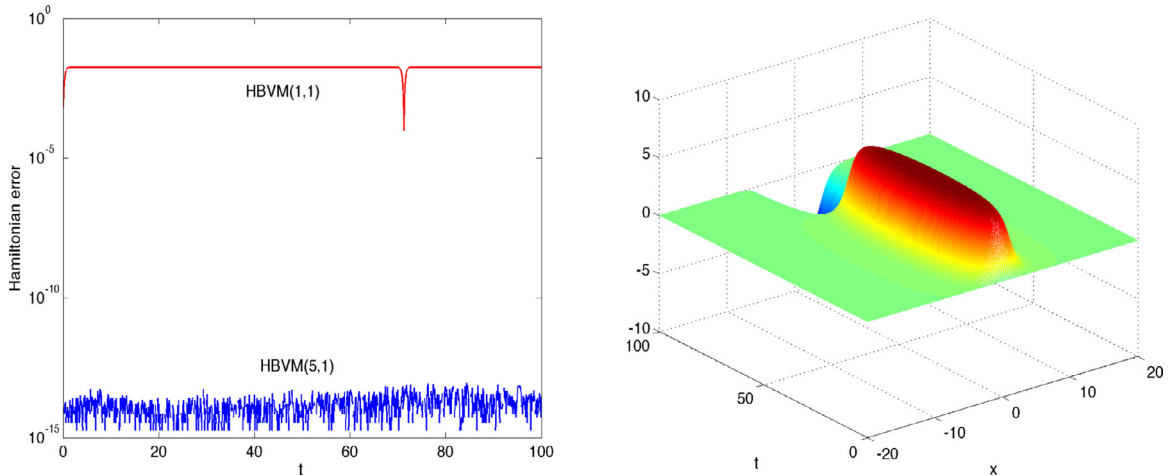
Fig. 3. Periodic boundary conditions and finite-difference approximation. Hamiltonian error (left plot) when using the HBVM(1,1) and HBVM(5,1) methods with stepsize $h = 0.1$, and numerical solution provided by HBVM(1,1) (right plot) when solving problem (101)–(102) with $\gamma = 1$.

is named *double-pole*, separates the two different types of dynamics and is shown in the left plot of Fig. 2. Moreover, the space interval being fixed,[11] the Hamiltonian is a decreasing function of γ, as is shown in the right plot of Fig. 2. This means that the value of the Hamiltonian characterizes the dynamics. Consequently, in a neighborhood of $\gamma = 1$, where the Hamiltonian assumes a value $\simeq 16$, nearby values of the Hamiltonian will provide different types of soliton solutions. As a result, energy conserving methods are expected to be useful, when numerically solving problem (101)–(102) with $\gamma = 1$. For this reason, in all the following experiments, the boundary conditions are prescribed in order to reproduce the solution (103) corresponding to $\gamma = 1$.

Let us then solve such a problem, at first with periodic boundary conditions, by using:

- A finite-difference approximation with $N = 400$ equispaced mesh points.
- A trigonometric polynomial approximation of degree $N = 100$ and, moreover, $m = 200$ equispaced mesh points.[12] In so doing, the error (87) in the initial condition is $e_N \simeq 1.6 \times 10^{-11}$, so that it is quite well matched.

For the time integration, let us consider the following second-order methods, used with stepsize $h = 10^{-1}$ for 10^3 integration steps:

- the (symplectic) implicit mid-point rule, i.e., HBVM(1,1), for which the Hamiltonian error is $\simeq 2 \times 10^{-2}$ (though without a drift);
- the (practically) energy-conserving HBVM(5,1) method, for which the Hamiltonian error is $\simeq 9 \times 10^{-14}$.

Concerning the finite-difference space approximation, the error in the numerical Hamiltonian is plotted on the left of Fig. 3. The right plot of the same figure illustrates the numerical approximation to the solution computed by the HBVM(1,1) method: as is clear, the computed approximation is wrong, since the method has provided a *breather*-like solution. On the contrary, HBVM(5,1) provides a correct approximation, qualitatively similar to that in the left-plot of Fig. 2: it is shown in the left plot in Fig. 5. It is worth mentioning that the value of the numerical Hamiltonian, in the case of the right plot of Fig. 3, is *lower* than the correct one, thus confirming that, according to the right plot in Fig. 2, it would correspond to an "artificial" larger value of γ.

Concerning the trigonometric polynomial approximation, the error in the numerical Hamiltonian is plotted on the left of Fig. 4. The right plot of the same figure illustrates the numerical approximation to the solution computed by the HBVM(1,1) method: it has again a *breather*-like shape and, thus, it is not qualitatively correct. On the contrary, HBVM(5,1) is able to reproduce the correct behavior of the solution, as is shown in the right plot in Fig. 5.

Completely similar results are obtained by using the same methods (and with the same stepsize h), when Dirichlet boundary conditions are prescribed for (101)–(102):

- On the left of Fig. 6, there is the plot of $H(\mathbf{q}_n, \mathbf{p}_n, t_n) - H(\mathbf{q}_0, \mathbf{p}_0, 0)$ (see (44)) and $\tilde{H}(\mathbf{q}_n, \mathbf{p}_n, \tilde{q}_n, \tilde{p}_n) - \tilde{H}(\mathbf{q}_n, \mathbf{p}_n, \tilde{q}_0, \tilde{p}_0)$ (see (48)), when using the HBVM(1,1) method. Both differences are quite large and almost overlapping. As a result, the computed numerical solution, shown in the right plot of Fig. 6, is wrong.
- On the left of Fig. 7, there is the plot of $H(\mathbf{q}_n, \mathbf{p}_n, t_n) - H(\mathbf{q}_0, \mathbf{p}_0, 0)$ (see (44)) and $\tilde{H}(\mathbf{q}_n, \mathbf{p}_n, \tilde{q}_n, \tilde{p}_n) - \tilde{H}(\mathbf{q}_n, \mathbf{p}_n, \tilde{q}_0, \tilde{p}_0)$ (see (48)), when using the HBVM(5,1) method. The augmented Hamiltonian (48) is now conserved, whereas the original Hamiltonian (44) undergoes small oscillations around its initial value. The computed solution, shown in the right plot of Fig. 7, is now correct.

---

[11] I.e., $[-20, 20]$, in our case (see (101)).
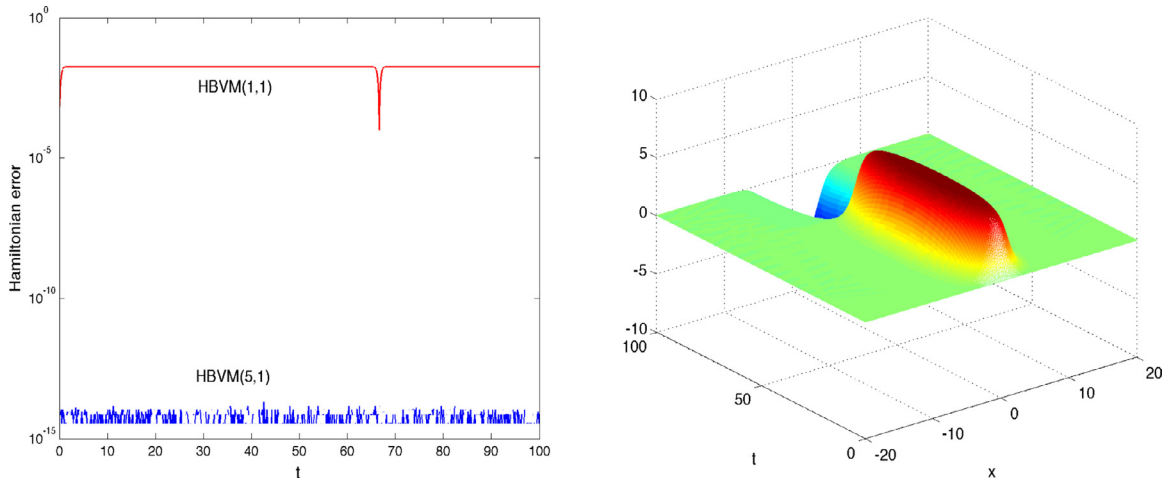[12] In fact, $m = 200$ is an appropriate choice for $N = 100$, in this case.

Fig. 4. Periodic boundary conditions and Fourier–Galerkin approximation. Hamiltonian error (left plot) when using the HBVM(1,1) and HBVM(5,1) methods with stepsize $h = 0.1$, and numerical solution provided by HBVM(1,1) (right plot) when solving problem (101)–(102) with $\gamma = 1$.
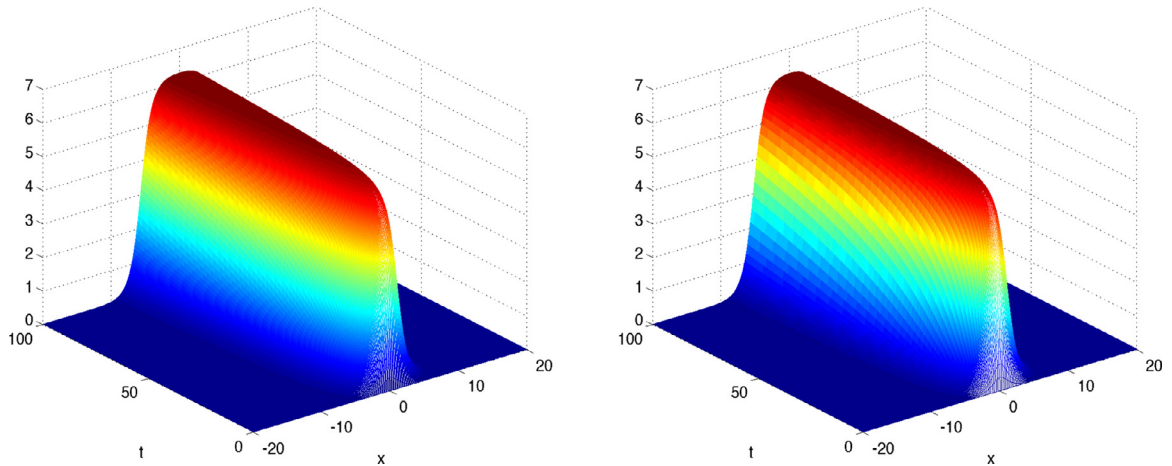

Fig. 5. Periodic boundary conditions. Computed solution by HBVM(5,1) with stepsize $h = 0.1$ by using a finite-difference spatial discretization (left plot) or a spectral space discretization (right plot).
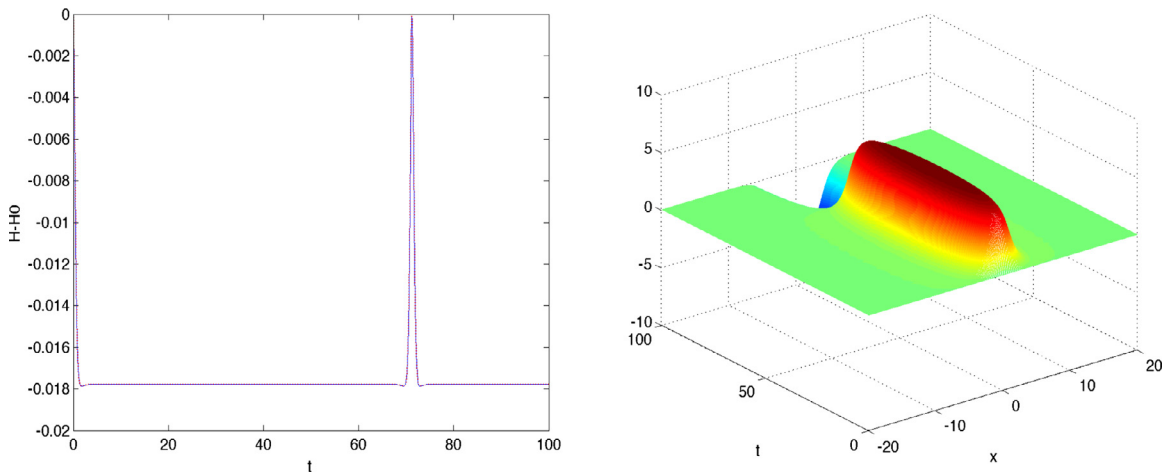

Fig. 6. Dirichlet boundary conditions. Difference with the initial value for the numerical Hamiltonian and augmented Hamiltonian (left plot) when solving problem (101)–(102) with $\gamma = 1$, by using HBVM(1,1) with stepsize $h = 0.1$, along with the computed solution (right plot).
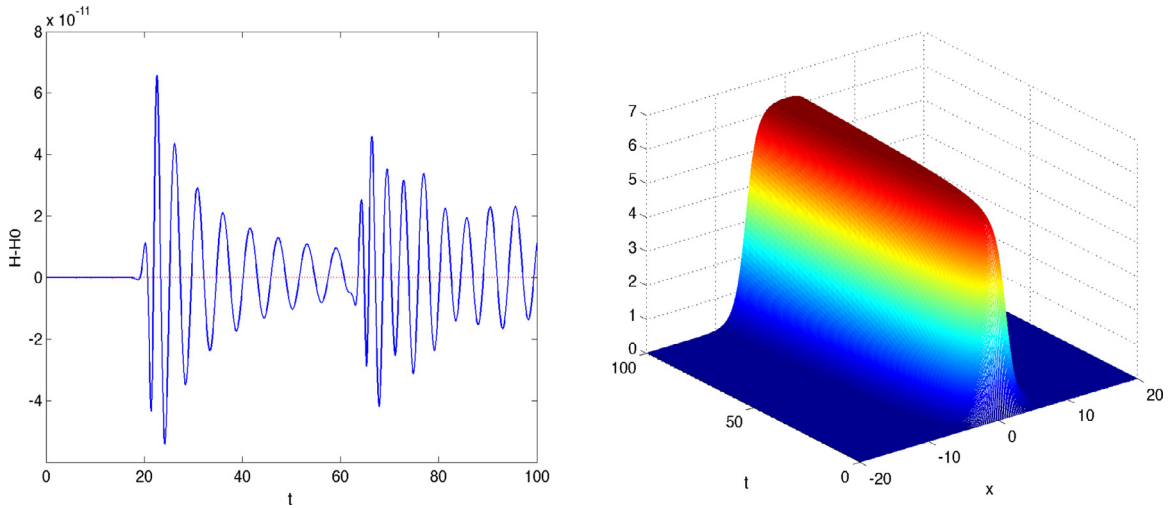
Fig. 7. Dirichlet boundary conditions. Difference with the initial value for the numerical Hamiltonian and augmented Hamiltonian (left plot) when solving problem (101)–(102) with $\gamma = 1$, by using HBVM(5,1) with stepsize $h = 0.1$, along with the computed solution (right plot).
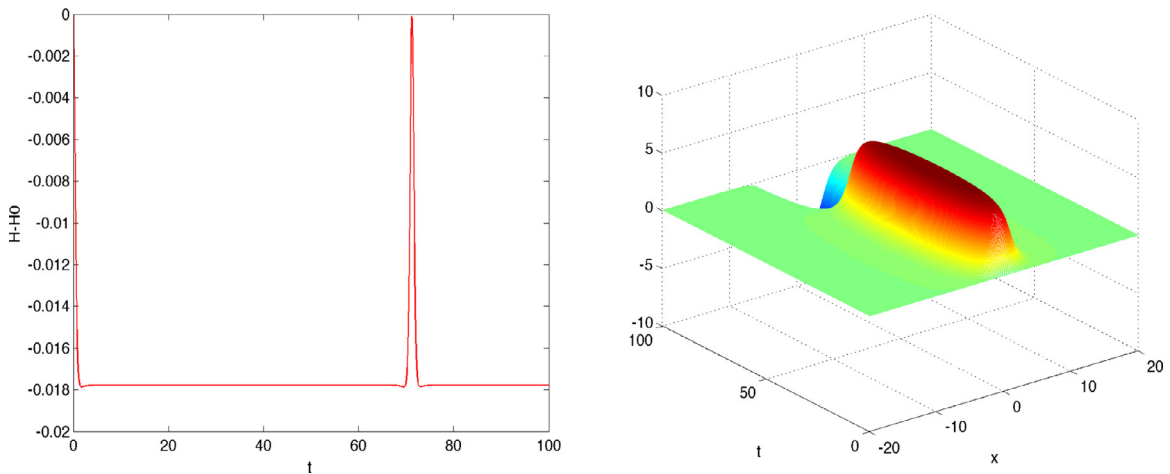

Fig. 8. Neumann boundary conditions. Difference with the initial value for the numerical Hamiltonian and augmented Hamiltonian (left plot) when solving problem (101)–(102) with $\gamma = 1$, by using HBVM(1,1) with stepsize $h = 0.1$, along with the computed solution (right plot).

Analogous results are obtained when Neumann boundary conditions are prescribed for (101)–(102). In fact, by considering the same methods and stepsize h:

- On the left of Fig. 8, there is the plot of $H(\mathbf{q}_n, \mathbf{p}_n, t_n) - H(\mathbf{q}_0, \mathbf{p}_0, 0)$ (see (60)) and $\tilde{H}(\mathbf{q}_n, \mathbf{p}_n, \tilde{q}_n, \tilde{p}_n) - \tilde{H}(\mathbf{q}_n, \mathbf{p}_n, \tilde{q}_0, \tilde{p}_0)$ (see (64)), when using the HBVM(1,1) method. Both of them are quite large and almost overlapping. As a result, the computed numerical solution, shown in the right plot of Fig. 8, is wrong.
- On the left of Fig. 9, there is the plot of $H(\mathbf{q}_n, \mathbf{p}_n, t_n) - H(\mathbf{q}_0, \mathbf{p}_0, 0)$ (see (60)) and $\tilde{H}(\mathbf{q}_n, \mathbf{p}_n, \tilde{q}_n, \tilde{p}_n) - \tilde{H}(\mathbf{q}_n, \mathbf{p}_n, \tilde{q}_0, \tilde{p}_0)$ (see (64)), when using the HBVM(5,1) method. The augmented Hamiltonian (64) is now conserved, whereas the original Hamiltonian (60) undergoes small oscillations around its initial value. The computed solution, shown in the right plot of Fig. 9, is now correct.

As one can see in the plots on the left in Figs. 7 and 9, since the boundary conditions are small, we have a very small variation of the semi-discrete Hamiltonian. Therefore, we are in the situation presented in Remark 4, and thus, even though the numerical solution computed by a HBVM(k, 1) method is only second order accurate in time, we expect the error in the Hamiltonian to decrease with order $2k$, until it reaches the same order of magnitude as the error on the $\tilde{p}$ component, according to (58). As an example, let us consider again problem (101)–(102) coupled with Dirichlet boundary conditions. In Fig. 11, we plot the errors on the solution (solid line), on the Hamiltonian H (dashed line) and on $\tilde{p}$ (dotted line with circles), at time $t = 100$, versus the time-step h, for HBVM(k, 1), $k = 1, 2, 3, 4$.

As one may see, the error on the solution always decreases with order 2, as well as the error on $\tilde{p}$ (which is quite small $\simeq 10^{-10} \equiv \varepsilon$). Differently, the error on the Hamiltonian decreases with order $2k$ as long as it is larger than the error on $\tilde{p}$. In
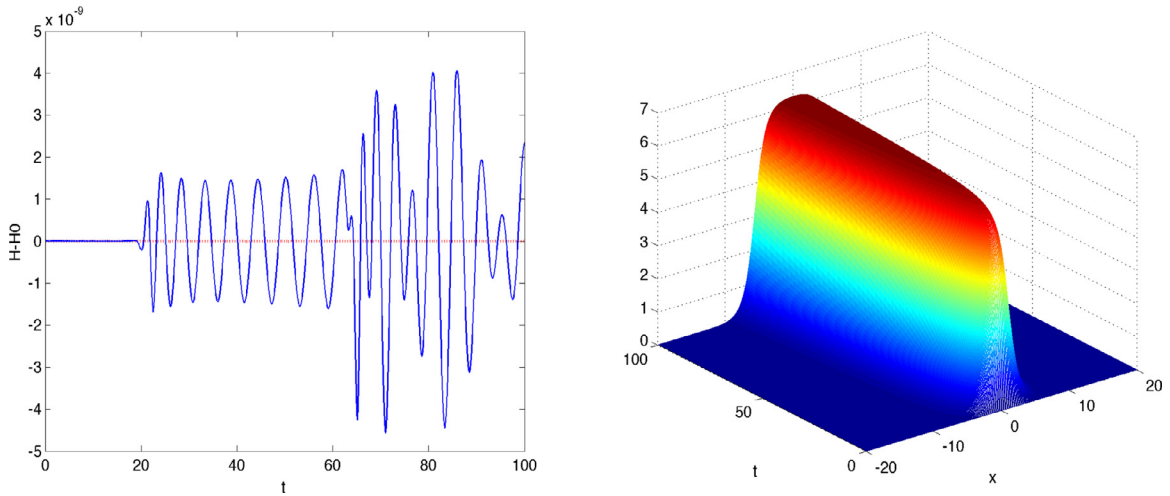
Fig. 9. Neumann boundary conditions. Difference with the initial value for the numerical Hamiltonian and augmented Hamiltonian (left plot) when solving problem (101)–(102) with $\gamma = 1$, by using HBVM(5,1) with stepsize $h = 0.1$, along with the computed solution (right plot).
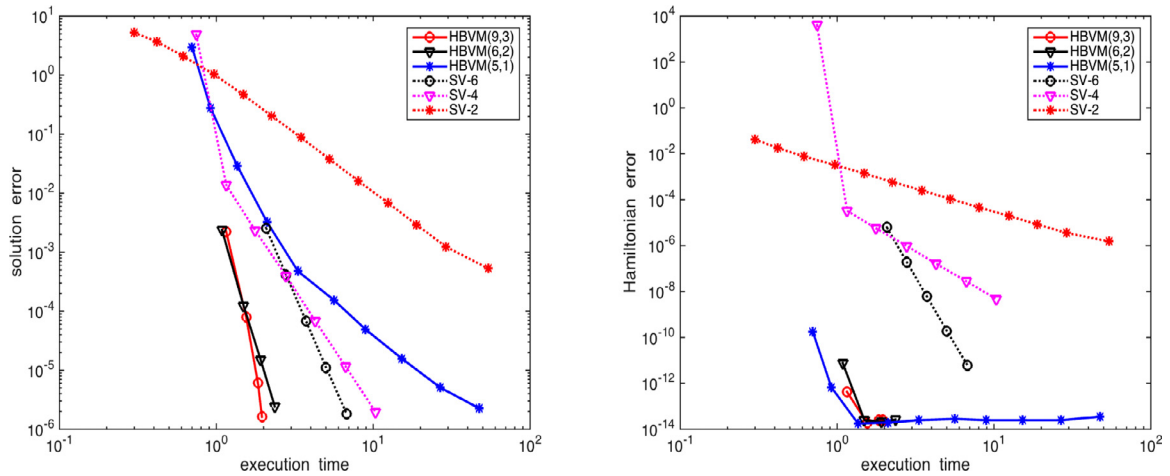

Fig. 10. *Work-Precision Diagram* (left plot) and Hamiltonian error versus execution time (right plot) for problem (101)–(102).

particular, for $k = 4$, the Hamiltonian error starts decreasing with order 8 (for $h > 0.25$), becoming soon comparable with the error on $\tilde{p}$ (for $h < 0.25$), and henceforth decreasing approximately with order 2.

We now highlight the potentialities of the Fourier–Galerkin space approximation, with respect to the finite-difference one, when periodic boundary conditions are prescribed for the problem: in fact, the Fourier approximation (86) to the Hamiltonian converges more than exponentially in the number N of Fourier modes, whereas the finite-difference approximation (23) converges only quadratically in Δx. Since also HBVM(5,1) is second order, we then compare the use of such a method, with stepsize $h = 40/\ell$ in time and for a total of ℓ time-steps, for solving problem (101)–(102), with $\gamma = 1$ and periodic boundary conditions, by using:

- The second-order finite-difference spatial discretization with ℓ mesh points (with this choice, one has $\Delta x = h$).
- The Fourier–Galerkin approximation with $N = 100$, and $m = 200$ spatial grid-points, which we maintain fixed independently of the choice of ℓ. This because the obtained spatial approximation yields a far more accurate approximation than the one corresponding to the time discretization.

Table 1 summarizes the obtained results: both methods are globally second-order accurate, even though the values of N and m are kept fixed in the second case (thus confirming the well known exponential convergence of the Fourier approximation). Moreover, by comparing the maximum error in the finite-difference case (FD-error) and in the Fourier–Galerkin approach (FG-error), one sees that the latter is much more favorable than the former.

As mentioned at the end of the previous section, we now compare several HBVM methods in terms of required nonlinear iterations to obtain the full convergence for problem (101)–(102), with $\gamma = 1$ and periodic boundary conditions on the time
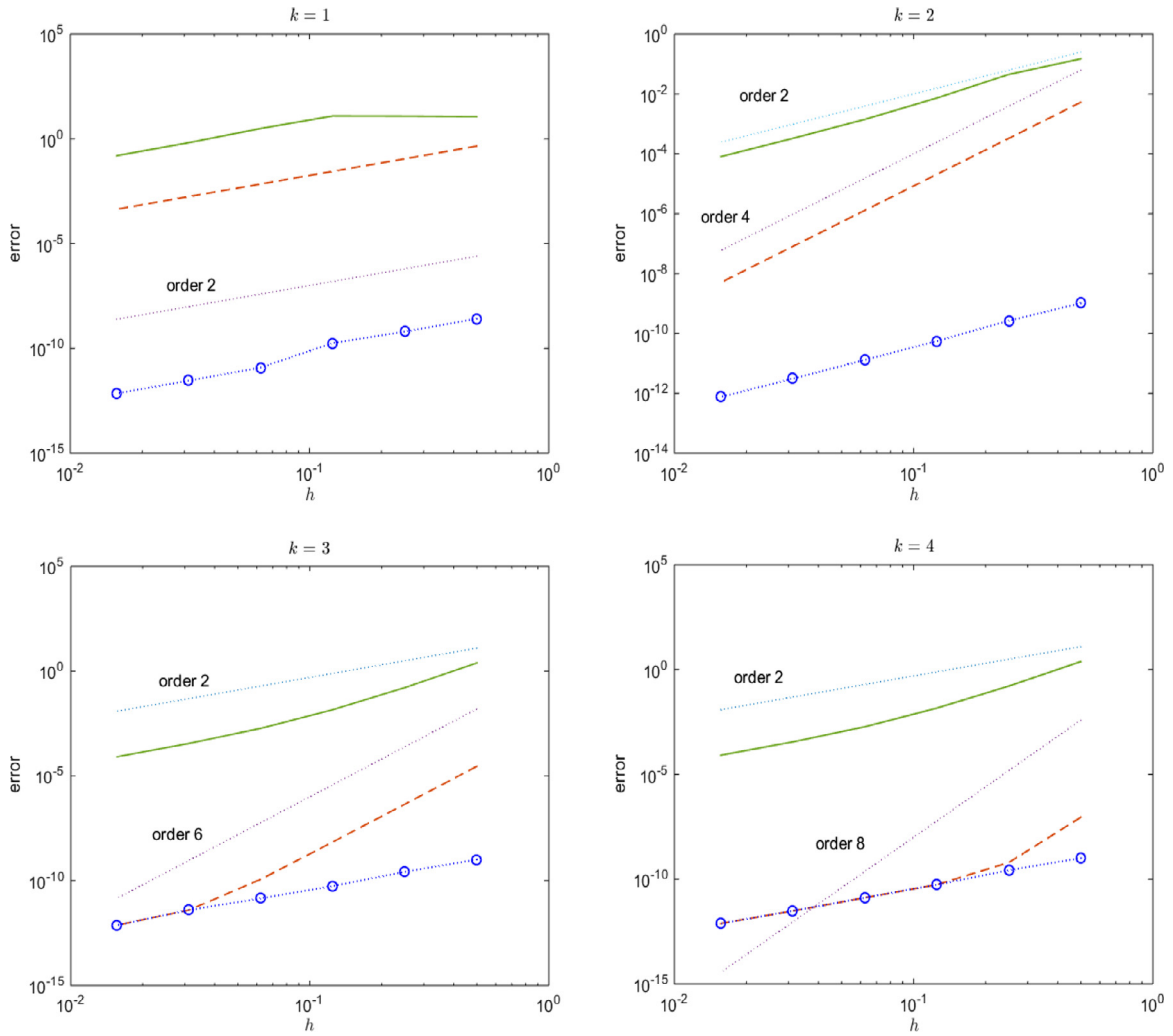
Fig. 11. Sine-Gordon problem (101)–(102) with $\gamma = 1$, Dirichlet boundary conditions and finite-difference semi-discretization with $N = 400$, solved by means of HBVM(k, 1), $k = 1, 2, 3, 4$. Errors at time $t = 100$ versus time-step for the solution (solid line), the Hamiltonian function H (dashed line) and $\tilde{p}$ (dotted line with circles).

Table 1
Comparing finite-difference (FD) and Fourier–Galerkin (FG) errors.

ℓ	FD-error	Rate	FG-error	Rate
400	1.4486e−01	–	1.7883e−03	–
800	3.6900e−02	1.97	4.4985e−04	1.99
1600	9.2702e−03	1.99	1.1262e−04	2.00
3200	2.3204e−03	2.00	2.8171e−05	2.00

interval [0, 100]. We consider the results for three different stepsizes: $h = 0.5, h = 0.1$ and $h = 0.01$.[13] As one can infer from comparing the figures in Tables 2–4 with the ones in Tables 5–7, respectively, the same HBVM in time requires a smaller number of iterations, when applied to the semi-discrete problem obtained by using a Fourier–Galerkin (FG) space discretization, than that required by using a finite-difference (FD) space discretization.[14] As a matter of fact, from the previous tables one deduces that, for $h = 0.5$, the mean number of iterations per step is approximately 21.7 for FG and 27.2 for FD; similarly, for $h = 0.1$ it is 5.8 for FG and 8.6 for FD; at last, for $h = 0.01$, it is approximately 3.1 for FG and 3.9 for FD. Moreover, if a spectral method is used

---

[13] I.e., a "large", a "medium" and a "small" stepsize, respectively, for the given spatial accuracy.

[14] This can be expected, since the approximate Jacobian is diagonal, in the former case, and tridiagonal, in the latter one.

Table 2
Iterations required by HBVM(k, s) for solving problem (101)–(102) with stepsize $h = 0.5$ and a Fourier–Galerkin discretization in space.

					k				
s	s	$s+1$	$s+2$	$s+3$	$s+4$	$s+5$	$s+6$	$s+7$	$s+8$
1	2200	2248	2291	2305	2312	2317	2321	2323	2316
2	3630	3648	3660	3664	3665	3667	3667	3669	3669
3	5206	5213	5221	5250	5303	5346	5368	5377	5381
4	6023	6049	6064	6093	6102	6114	6122	6135	6138

Table 3
Iterations required by HBVM(k, s) for solving problem (101)–(102) with stepsize $h = 0.1$ and a Fourier–Galerkin discretization in space.

					k				
s	s	$s+1$	$s+2$	$s+3$	$s+4$	$s+5$	$s+6$	$s+7$	$s+8$
1	5047	5120	5129	5130	5131	5135	5139	5139	5139
2	6280	6384	6457	6513	6550	6569	6593	6615	6626
3	5639	5802	5802	5765	5807	5804	5800	5808	5802
4	5469	5527	5556	5570	5585	5605	5613	5621	5624

Table 4
Iterations required by HBVM(k, s) for solving problem (101)–(102) with stepsize $h = 0.01$ and a Fourier–Galerkin discretization in space.

					k				
s	s	$s+1$	$s+2$	$s+3$	$s+4$	$s+5$	$s+6$	$s+7$	$s+8$
1	30,000	30,489	30,519	30,530	30,534	30,540	30,541	30,544	30,546
2	30,687	30,796	30,845	30,869	30,883	30,889	30,902	30,908	30,906
3	30,304	30,335	30,343	30,334	30,340	30,343	30,336	30,341	30,341
4	30,294	30,322	30,338	30,347	30,353	30,357	30,359	30,363	30,366

Table 5
Iterations required by HBVM(k, s) for solving problem (101)–(102) with stepsize $h = 0.5$ and a finite-difference space discretization.

					k				
s	s	$s+1$	$s+2$	$s+3$	$s+4$	$s+5$	$s+6$	$s+7$	$s+8$
1	2366	2986	2982	3017	3030	3052	3034	3029	3040
2	4498	4520	4514	4538	4573	4567	4563	4589	4585
3	6421	6513	6549	6584	6590	6666	6651	6686	6702
4	7513	7599	7622	7628	7642	7686	7726	7759	7736

Table 6
Iterations required by HBVM(k, s) for solving problem (101)–(102) with stepsize $h = 0.1$ and a finite-difference space discretization.

					k				
s	s	$s+1$	$s+2$	$s+3$	$s+4$	$s+5$	$s+6$	$s+7$	$s+8$
1	5155	7708	7800	7843	7813	7701	7547	7395	7144
2	10,638	10,312	9825	9485	9262	9135	9073	9037	9029
3	9441	9201	9083	9031	8976	8949	8950	8942	8945
4	8429	8279	8265	8224	8200	8179	8187	8160	8128

Table 7
Iterations required by HBVM(k, s) for solving problem (101)–(102) with stepsize $h = 0.01$ and a finite-difference space discretization.

					k				
s	s	$s+1$	$s+2$	$s+3$	$s+4$	$s+5$	$s+6$	$s+7$	$s+8$
1	30,193	39,999	40,000	40,000	40,000	40,000	40,000	40,000	40,000
2	39,993	39,998	39,998	40,000	40,000	40,000	40,000	40,000	40,000
3	38,453	38,914	38,815	38,895	38,982	39,026	39,067	39,093	39,144
4	39,185	39,441	39,491	39,619	39,681	39,739	39,783	37,983	39,823

Table 8
Parameters used for constructing the plots in Fig. 10.

Method	h_{max}	h_{min}	ν_h
HBVM(5,1)	0.5	0.003	10
HBVM(6,2)	0.5	0.1	4
HBVM(9,3)	1	0.25	4
SV2	0.1	0.0006	13
SV4	0.1	0.007	7
SV6	0.1	0.01	5

in space, the number of required iterations, for fixed s, is essentially independent of k. In particular, for the smallest considered stepsize, from the figures in Table 4 one sees that the number of iterations is approximately independent of both k and s.

Tables 5–7 show that, when a finite-difference method space discretization is used, more significant variations may occur as k changes, for a fixed s (in particular when $s = 1$). Nevertheless, increasing k may also result in a decrease of the required iterations, as one can see in Table 6, for $s > 1$. Table 7 shows that also in this case, excluding HBVM(1, 1), the number of required iteration for the smallest considered stepsize is essentially independent of both k and s.

We complete this section by performing a further numerical experiment, where we compare some (practically) energy-conserving HBVMs, with well known explicit methods of the same order, for solving problem (101)–(102), with $\gamma = 1$ and periodic boundary conditions, on the time interval [0, 100]. For all methods, a Fourier–Galerkin space discretization with $N = 100$, and $m = 200$ spatial grid-points, has been considered. In more details, we compare the following methods:

order 2: the (practically) energy-conserving HBVM(5,1) method, and the symplectic Störmer–Verlet method (SV2);
order 4: the (practically) energy-conserving HBVM(6,2) method, and the composition method (SV4) based on the symplectic Störmer–Verlet method (each step requiring three steps of the basic method), according to [49, p. 44];
order 6: the (practically) energy-conserving HBVM(9,3) method, and the composition method (SV6) based on the symplectic Störmer–Verlet method (each step requiring nine steps of the basic method), according to [49, p. 44].

To compare the methods, we construct a corresponding *Work-Precision Diagram*, by following the standard used in the *Test Set for IVP Solvers* [84]. In more details, we plot the accuracy, measured in terms of the maximum absolute error, w.r.t. the execution time. All tests have been done by using Matlab v. 2014b, running on a dual core i7 at 2.8 GHz computer with 8GB of memory. The curve of each method is obtained by using ν_h (logarithmically) equispaced steps between h_{min} and h_{max}, as specified in Table 8.[15] When the stepsize used does not exactly divide the final time $T = 100$, the nearest mesh-point is considered.

The left plot in Fig. 10 summarizes the obtained results, and one sees that the (practically) energy-conserving HBVMs are competitive, even w.r.t. explicit solvers of the same order. For sake of completeness, on the right in Fig. 10, we plot the corresponding Hamiltonian error versus the execution time, thus confirming that HBVMs are practically energy conserving also for non polynomial Hamiltonians: in fact, taking aside the coarser time-steps, all methods have a Hamiltonian error which is within roundoff errors. On the contrary, for the other methods the decrease of the Hamiltonian error matches their order.

8. Conclusions

In this paper, we have compared the conservation properties of the semilinear wave equation with the corresponding ones obtained after semi-discretization of the space variable, both when considering a finite-difference and a spectral space discretization. When a finite-difference space discretization is considered, we have also studied the case when non-periodic boundary conditions are prescribed for the problem.

The conservation properties of the semi-discrete problem can be conveniently inherited by the numerical solution provided by energy-conserving methods in the HBVMs class. Such methods turn out to be computationally appealing, since they result to be competitive even w.r.t. explicit methods, and allow a safer approximation of the solution, when energy conservation is an issue, as is confirmed by a few numerical tests on the sine-Gordon equation with a soliton-like solution.

The arguments can be extended in a quite straightforward way to other Hamiltonian partial differential equations, e.g., the Schrödinger equation (as is sketched in the Appendix), which will be the subject of future investigations. Also a more comprehensive study of Fourier–Galerkin space semi-discretization, when non periodic boundary conditions are prescribed, will be considered in future investigations.

A further direction of research will concern the conservation of multiple invariants for the semi-discrete problem, by means of arguments similar to those used in [14,25].

---

[15] Larger values of h_{max} for the explicit methods (see Table 8) are not allowed because of stability reasons.

Appendix

We here sketch the basic facts that allow an extension of the analysis carried out for the semilinear wave equation (1), to different Hamiltonian PDEs. In particular, we here consider the nonlinear Schrödinger equation (in dimensionless form),

$$i\psi_t + \psi_{xx} + 2\kappa |\psi|^2 \psi = 0, \quad (x,t) \in (0,1) \times (0,\infty), \quad \psi(x,0) \quad \text{given}, \tag{104}$$

where i denotes, as usual, the imaginary unit. By setting

$$\psi = u + iv,$$

one then obtains the real form of (104),

$$
\begin{aligned}
u_t &= -v_{xx} - 2\kappa (u^2 + v^2) v, \quad (x,t) \in (0,1) \times (0,\infty), \\
v_t &= u_{xx} + 2\kappa (u^2 + v^2) u,
\end{aligned}
\tag{105}
$$

which is Hamiltonian with Hamiltonian (compare with (7))

$$\mathcal{H}[u,v](t) = \frac{1}{2} \int_0^1 [u_x^2(x,t) + v_x^2(x,t) - \kappa (u^2(x,t) + v^2(x,t))^2] \mathrm{d}x \equiv \int_0^1 E(x,t)\, \mathrm{d}x. \tag{106}$$

In fact, (105) can be formally recast as in (8)–(10), with the new Hamiltonian functional (106). In order to be able to repeat for (105) the arguments seen for the Hamiltonian semi-discretization of (1), with either periodic, or Dirichlet, or Neumann boundary conditions, it is enough to derive the conservation law corresponding to (13) and the analogous of (36). Concerning the former conservation law, from (106) and (105) one obtains:

$$
\begin{aligned}
E_t(x,t) &= u_x(x,t)u_{xt}(x,t) + v_x(x,t)v_{xt}(x,t) - \overbrace{2\kappa \big(u^2(x,t) + v^2(x,t)\big)u(x,t)}^{=\,v_t - u_{xx}}\, u_t(x,t) \\
&\quad \underbrace{-2\kappa \big(u^2(x,t) + v^2(x,t)\big)v(x,t)}_{=\,u_t + v_{xx}}\, v_t(x,t) \\
&= u_x(x,t)u_{xt}(x,t) + u_t(x,t)u_{xx}(x,t) + v_x(x,t)v_{xt}(x,t) + v_t(x,t)v_{xx}(x,t) \\
&= (u_x(x,t)u_t(x,t))_x + (v_x(x,t)v_t(x,t))_x \equiv -F_x(x,t).
\end{aligned}
$$

Consequently, in place of (13) one obtains:

$$E_t(x,t) + F_x(x,t), \quad F(x,t) = -u_x(x,t)u_t(x,t) - v_x(x,t)v_t(x,t).$$

Similarly, taking into account (106) and (105), the analogous of (36) is given by:

$$
\begin{aligned}
\mathcal{H}[u,v](t) &= \frac{1}{2} \int_0^1 [u_x^2(x,t) + v_x^2(x,t) - \kappa (u^2(x,t) + v^2(x,t))^2] \mathrm{d}x \\
&= \frac{1}{2} \int_0^1 [-u(x,t)u_{xx}(x,t) + (u(x,t)u_x(x,t))_x - v(x,t)v_{xx}(x,t) + (v(x,t)v_x(x,t))_x - \kappa (u^2(x,t) + v^2(x,t))^2] \mathrm{d}x \\
&= -\frac{1}{2} \int_0^1 [u(x,t)u_{xx}(x,t) + v(x,t)v_{xx}(x,t) + \kappa (u^2(x,t) + v^2(x,t))^2] \mathrm{d}x \\
&\quad + \frac{1}{2} [u(1,t)u_x(1,t) - u(0,t)(t)u_x(0,t) + v(1,t)v_x(1,t) - v(0,t)(t)v_x(0,t)].
\end{aligned}
$$

The arguments for the Hamiltonian semi-discretization of (105) can then be repeated, *mutatis mutandis*, almost verbatim as seen for (1), both when considering a finite-difference and a Fourier–Galerkin space approximation.

References

[1] P. Amodio, L. Brugnano, F. Iavernaro, Energy-conserving methods for Hamiltonian boundary value problems and applications in astrodynamics, Adv. Comput. Math. doi:10.1007/s10444-014-9390-z.
[2] P. Amodio, I. Sgura, High-order finite difference schemes for the solution of second-order BVPs, J. Comput. Appl. Math. 176 (2005) 59–76.
[3] P. Betsch, P. Steinmann, Inherently energy conserving time finite elements for classical mechanics, J. Comput. Phys. 160 (1) (2000) 88–116.
[4] P. Betsch, P. Steinmann, Conservation properties of a time FE method. I. Time-stepping schemes for *N*-body problems, Int. J. Numer. Methods Eng. 49 (5) (2000) 599–638.
[5] J.P. Boyd, Chebyshev and Fourier Spectral Methods, second ed., Dover Publications Inc., Mineola, NY, 2001.
[6] T.J. Bridges, Multisymplectic structures and wave propagation, Math. Proc. Camb. Philos. Soc. 121 (1997) 147–190.
[7] T.J. Bridges, S. Reich, Multi-symplectic integrators: numerical schemes for Hamiltonian PDEs that conserve symplecticity, Phys. Lett. A 284 (2001) 184–193.
[8] T.J. Bridges, S. Reich, Multi-symplectic spectral discretizations for the Zakharov–Kuznetsov and shallow water equations, Physica D 152 (2001) 491–504.
[9] T.J. Bridges, S. Reich, Numerical methods for Hamiltonian PDEs, J. Phys. A: Math. Gen. 39 (2006) 5287–5320.
[10] L. Brugnano, Blended block BVMs (B3VMs): a family of economical implicit methods for ODEs, J. Comput. Appl. Math. 116 (2000) 41–62.
[11] L. Brugnano, M. Calvo, J.I. Montijano, L. Ràndez, Energy preserving methods for Poisson systems, J. Comput. Appl. Math. 236 (2012) 3890–3904.
[12] L. Brugnano, G. Frasca Caccia, F. Iavernaro, Efficient implementation of Gauss collocation and Hamiltonian Boundary Value Methods, Numer. Algor. 65 (2014) 633–650.

[13] L. Brugnano, G. Frasca Caccia, F. Iavernaro, Efficient implementation of geometric integrators for separable Hamiltonian problems, AIP Conf. Proc. 1558 (2013) 734–737.
[14] L. Brugnano, F. Iavernaro, Line Integral Methods which preserve all invariants of conservative problems, J. Comput. Appl. Math. 236 (2012) 3905–3919.
[15] L. Brugnano, F. Iavernaro, D. Trigiante, Analysis of Hamiltonian Boundary Value Methods (HBVMs): a class of energy-preserving Runge–Kutta methods for the numerical solution of polynomial Hamiltonian systems, Commun. Nonlin. Sci. Numer. Simul. 20 (2015) 650–667.
[16] L. Brugnano, F. Iavernaro, D. Trigiante, Hamiltonian BVMs (HBVMs): a family of "drift-free" methods for integrating polynomial Hamiltonian systems, AIP Conf. Proc. 1168 (2009) 715–718.
[17] L. Brugnano, F. Iavernaro, D. Trigiante, Hamiltonian Boundary Value Methods (energy preserving discrete line methods), J. Numer. Anal. Ind. Appl. Math. 5 (1–2) (2010) 17–37.
[18] L. Brugnano, F. Iavernaro, D. Trigiante, A note on the efficient implementation of Hamiltonian BVMs, J. Comput. Appl. Math. 236 (2011) 375–383.
[19] L. Brugnano, F. Iavernaro, D. Trigiante, The lack of continuity and the role of infinite and infinitesimal in numerical methods for ODEs: the case of symplecticity, Appl. Math. Comput. 218 (2012) 8053–8063.
[20] L. Brugnano, F. Iavernaro, D. Trigiante, A simple framework for the derivation and analysis of effective one-step methods for ODEs, Appl. Math. Comput. 218 (2012) 8475–8485.
[21] L. Brugnano, F. Iavernaro, D. Trigiante, A two-step, fourth-order method with energy preserving properties, Comput. Phys. Commun. 183 (2012) 1860–1868.
[22] L. Brugnano, F. Iavernaro, D. Trigiante, Energy and quadratic invariants preserving integrators based upon Gauss collocation formulae, SIAM J. Numer. Anal. 50 (6) (2012) 2897–2916.
[23] L. Brugnano, C. Magherini, Blended implementation of block implicit methods for ODEs, Appl. Numer. Math. 42 (2002) 29–45.
[24] L. Brugnano, C. Magherini, The BIM code for the numerical solution of ODES, J. Comput. Appl. Math. 164–165 (2004) 145–158.
[25] L. Brugnano, Y. Sun, Multiple invariants conserving Runge–Kutta type methods for Hamiltonian problems, Numer. Algor. 65 (2014) 611–632.
[26] B. Cano, Conserved quantities of some Hamiltonian wave equations after full discretization, Numer. Math. 103 (2006) 197–223.
[27] C. Canuto, M.Y. Hussaini, A. Quarteroni, T.A. Zang, Spectral Methods in Fluid Dynamics, Springer-Verlag, New York, 1988.
[28] M. Carpenter, D. Gottlieb, S. Abarbanel, Time-stable boundary conditions for finite-difference schemes solving hyperbolic systems: methodology and application to high-order compact schemes, J. Comp. Phys. 111 (1994) 220–236.
[29] E. Celledoni, V. Grimm, R.I. McLachlan, D.I. McLaren, D. O'Neale, B. Owren, G.R.W. Quispel, Preserving energy resp. dissipation in numerical PDEs using the "average vector field" method, J. Comput. Phys. 231 (20) (2012) 6770–6789.
[30] E. Celledoni, R.I. McLachlan, D.I. McLaren, B. Owren, G.R.W. Quispel, W.M. Wright, Energy-preserving Runge–Kutta methods, M2AN Math. Model. Numer. Anal. 43 (4) (2009) 645–649.
[31] E. Celledoni, B. Owren, Y. Sun, The minimal stage, energy preserving Runge–Kutta method for polynomial Hamiltonian systems is the averaged vector field method, Math. Comp. 83 (288) (2014) 1689–1700.
[32] J.B. Chen, M.Z. Qin, Multi-symplectic Fourier pseudospectral method for the nonlinear Schrödinger equation, Electron. Trans. Numer. Anal. 12 (2001) 193–204.
[33] D. Cohen, E. Hairer, C. Lubich, Conservation of energy, momentum and actions in numerical discretizations of non-linear wave equations, Numer. Math. 110 (2008) 113–143.
[34] G. Dahlquist, Å. Björk, Numerical Methods in Scientific Computing, vol. 1, SIAM, Philadelphia, 2008.
[35] G.A. Evans, J.R. Webster, A comparison of some methods for the evaluation of highly oscillatory integrals, J. Comput. Appl. Math. 112 (1999) 55–69.
[36] L.C. Evans, Partial Differential Equations, second ed., AMS, 2010.
[37] E. Faou, Geometric Numerical Integration and Schrödinger Equations, Zurich Lectures in Advanced Mathematics, European Mathematical Society (EMS), Zürich, 2012.
[38] T. Flå, A numerical energy conserving method for the DNLS equation, J. Comput. Phys. 101 (1992) 71–79.
[39] B. Forneberg, G.B. Whitham, A numerical and theoretical study of certain nonlinear wave phenomena, Proc. R. Soc. Lond. A 289 (1978) 373–403.
[40] J. Frank, Conservation of wave action under multisymplectic discretizations, J. Phys. A: Math. Gen. 39 (2006) 5479–5493.
[41] J. Frank, B.E. Moore, S. Reich, Linear PDEs and numerical methods that preserve a multisymplectic conservation law, SIAM J. Sci. Comput. 28 (2006) 260–277.
[42] J. de Frutos, T. Ortega, J.M. Sanz-Serna, A Hamiltonian, explicit algorithm with spectral accuracy for the "good" Boussinesq system, Comput. Methods Appl. Mech. Eng. 80 (1990) 417–423.
[43] D. Funaro, D. Gottlieb, A new method of imposing boundary conditions for hyperbolic equations, Math. Comp. 51 (1988) 599–613.
[44] D. Furihata, Finite-difference schemes for nonlinear wave equation that inherit energy conservation property, J. Comput. Appl. Math. 134 (1–2) (2001) 37–57.
[45] D. Furihata, T. Matsuo, Discrete Variational Derivative Method. A Structure-preserving Numerical Method for Partial Differential Equations, CRC Press, Boca Raton, FL, 2011.
[46] B. Gustafsson, High Order Difference Methods for Time Dependent PDE, Springer-Verlag, Berlin, 2008.
[47] E. Hairer, Energy-preserving variant of collocation methods, JNAIAM J. Numer. Anal. Ind. Appl. Math. 5 (1–2) (2010) 73–84.
[48] M. Huang, A Hamiltonian approximation to simulate solitary waves of the Kortweg–de Vries equation, Math. Comp. 56 (194) (1991) 607–620.
[49] E. Hairer, C. Lubich, G. Wanner, Geometric Numerical Integration. Structure-preserving Algorithms for Ordinary Differential Equations, second ed., Springer-Verlag, Berlin, 2006.
[50] E. Hairer, C. Lubich, Spectral semi-discretisations of weakly nonlinear wave equations over long times, Found. Comput. Math. 8 (2008) 319–334.
[51] B.M. Herbst, M.J. Ablowitz, Numerical chaos, symplectic integrators, and exponentially small splitting distances, J. Comput. Phys. 105 (1) (1993) 122–132.
[52] W. Hu, Z. Deng, S. Han, W. Zhang, Generalized multi-symplectic integrators for a class of Hamiltonian nonlinear wave PDEs, J. Comput. Phys. 235 (2013) 394–406.
[53] S. Koide, D. Furihata, Nonlinear and linear conservative finite difference schemes for regularized long wave equation, Jpn. J. Ind. Appl. Math. 26 (1) (2009) 15–40.
[54] F. Iavernaro, B. Pace, s-Stage trapezoidal methods for the conservation of Hamiltonian functions of polynomial type, AIP Conf. Proc. 936 (2007) 603–606.
[55] F. Iavernaro, B. Pace, Conservative block-boundary value methods for the solution of polynomial Hamiltonian systems, AIP Conf. Proc. 1048 (2008) 888–891.
[56] F. Iavernaro, D. Trigiante, High-order symmetric schemes for the energy conservation of polynomial Hamiltonian problems, J. Numer. Anal. Ind. Appl. Math. 4 (1–2) (2009) 87–101.
[57] A.L. Islas, C.M. Schober, On the preservation of phase space structure under multisymplectic discretization, J. Comput. Phys. 197 (2) (2004) 585–609.
[58] A.L. Islas, C.M. Schober, Backward error analysis for multisymplectic discretizations of Hamiltonian PDEs, Math. Comput. Simul. 69 (2005) 290–303.
[59] A.L. Islas, C.M. Schober, Conservation properties of multisymplectic integrators, Future Generation Comput. Syst. 22 (2006) 412–422.
[60] A. Kurganov, J. Rauch, et al., The order of accuracy of quadrature formulae for periodic functions, in: A. Bove, et al. (Eds.), Advances in Phase Space Analysis of Partial Differential Equations, Birkhäuser, Boston, 2009.
[61] R.I. McLachlan, G.R.W. Quispel, Discrete gradient methods have an energy conservation law, Discrete Contin. Dyn. Syst. 34 (3) (2014) 1099–1104.
[62] R.I. McLachlan, G.R.W. Quispel, N. Robidoux, Geometric integration using discrete gradient, Philos. Trans. R. Soc. Lond. A 357 (1999) 1021–1045.
[63] M.P. Laburta, J.I. Montijano, L. Rández, M. Calvo, Numerical methods for non conservative perturbations of conservative problems, Comput. Phys. Commun. 187 (2015) 72–82.
[64] B. Leimkulher, S. Reich, Simulating Hamiltonian Dynamics, Cambridge University Press, 2004.
[65] C.W. Li, M.Z. Qin, A symplectic difference scheme for the infinite-dimensional Hamilton system, J. Comput. Math. 6 (1988) 164–174.
[66] S. Li, L. Vu-Quoc, Finite difference calculus invariant structure of a class of algorithms for the nonlinear Klein–Gordon equation, SIAM J. Numer. Anal. 32 (1995) 1839–1875.
[67] X. Lu, R. Schmid, A symplectic algorithm for wave equations, Math. Comput. Simul. 43 (1997) 29–38.

[68] J.E. Marsden, G.P. Patrick, S. Shkoller, Multi-symplectic geometry, variational integrators, and nonlinear PDEs, Commun. Math. Phys. 199 (1999) 351–395.
[69] T. Matsuo, New conservative schemes with discrete variational derivatives for nonlinear wave equations, J. Comput. Appl. Math. 203 (2007) 32–56.
[70] T. Matsuo, M. Sugihara, D. Furihata, M. Mori, Spatially accurate dissipative or conservative finite difference schemes derived by the discrete variational method, Jpn. J. Ind. Appl. Math. 19 (3) (2002) 311–330.
[71] K. Mattsson, J. Nordström, Summation by parts operators for finite difference approximations of second derivatives, J. Comp. Phys. 199 (2004) 503–540.
[72] B. Moore, S. Reich, Backward error analysis for multi-symplectic integration methods, Numer. Math. 95 (2003) 625–652.
[73] M. Oliver, M. West, C. Wulff, Approximate momentum conservation for spatial semidiscretization of semilinear wave equations, Numer. Math. 97 (2004) 493–535.
[74] P. Olsson, Summation by parts, projections, and stability: I, Math. Comp. 64 (1995) 1035–1065.
[75] P. Olsson, Summation by parts, projections, and stability: I, Math. Comp. 64 (1995) 1473–1493.
[76] M.-Z. Qin, M.-Q. Zhang, Multi-stage symplectic schemes of two kinds of Hamiltonian systems for wave equations, Comput. Math. Appl. 19 (10) (1990) 51–62.
[77] G.R.W. Quispel, D.I. McLaren, A new class of energy-preserving numerical integration methods, J. Phys. A 41 (045206) (2008) 7.
[78] J.M. Sanz-Serna, M.P. Calvo, Numerical Hamiltonian Problems, Chapman & Hall, 1994.
[79] B. Strand, Summation by parts for finite difference approximations for d/dx, J. Comp. Phys. 110 (1994) 47–67.
[80] W. Strauss, L. Vázquez, Numerical solution of a nonlinear Klein–Gordon equation, J. Comput. Phys. 28 (1978) 271–278.
[81] J. Wang, A note on multisymplectic Fourier pseudospectral discretization for the nonlinear Schrödinger equation, Appl. Math. Comput. 191 (2007) 31–41.
[82] S.B. Wineberg, J.F.M. Grath, E.F. Gabl, L.R. Scott, C.E. Southwell, Implicit spectral methods for wave propagation problems, J. Comp. Phys. 97 (1991) 311–336.
[83] T.H. Wlodarczyk, Stability and Preservation Properties of Multisymplectic Integrators (Ph.D. thesis), Department of Mathematics in the College of Sciences at the University of Central Florida, Orlando, Florida, 2007. http://etd.fcla.edu/CF/CFE0001817/Wlodarczyk_Tomasz_H_200708_PhD.pdf
[84] https://www.dm.uniba.it/~testset/testsetivpsolvers/.